



HAL
open science

Thermodynamic modelling of the Ca–O system including 3rd generation description of CaO and CaO₂

Guillaume Deffrennes, Noël Jakse, Cecilia M.S. Alvares, Ioana Nuta, Alain Pasturel, Alexandra Khvan, Alexander Pisch

► **To cite this version:**

Guillaume Deffrennes, Noël Jakse, Cecilia M.S. Alvares, Ioana Nuta, Alain Pasturel, et al.. Thermodynamic modelling of the Ca–O system including 3rd generation description of CaO and CaO₂. Calphad, 2020, 69, pp.101764. 10.1016/j.calphad.2020.101764 . hal-02559067

HAL Id: hal-02559067

<https://hal.science/hal-02559067>

Submitted on 30 Apr 2020

HAL is a multi-disciplinary open access archive for the deposit and dissemination of scientific research documents, whether they are published or not. The documents may come from teaching and research institutions in France or abroad, or from public or private research centers.

L'archive ouverte pluridisciplinaire **HAL**, est destinée au dépôt et à la diffusion de documents scientifiques de niveau recherche, publiés ou non, émanant des établissements d'enseignement et de recherche français ou étrangers, des laboratoires publics ou privés.

Thermodynamic modelling of the Ca-O system including 3rd generation description of CaO and CaO₂

Guillaume Deffrennes^a, Noël Jakse^a, Cecilia M. S. Alvares^a, Ioana Nuta^a, Alain Pasturel^a, Alexandra Khvan^b, Alexander Pisch^a

^aUniv. Grenoble Alpes, CNRS, Grenoble INP, SIMaP, F-38000 Grenoble, France

^bThermochemistry of Materials SRC, NUST MISIS, Leninskiy prosp 4, 119049 Moscow, Russia

Corresponding author: Dr. Alexander Pisch

Postal address : SIMaP 1130 Rue de la Piscine BP 75 38402 St. Martin d'Hères Cedex

Tel. : 0476826510

Fax : 0476826663

Keywords : Ca – O, Calcium oxide, CALPHAD modelling, thermodynamic assessment, 3rd generation CALPHAD database

Abstract

A complete thermodynamic description of the Ca – O system is proposed including 3rd generation modelling of crystalline CaO, liquid and amorphous CaO, and crystalline CaO₂. Compared to previous modellings, a more robust description of the thermodynamic properties of the binary phases is achieved using data recently obtained by density functional theory calculations and molecular dynamics simulations. The heat capacity of crystalline CaO is reassessed, leading to a noticeably higher value below the melting point compared to previous modellings and resulting in a slightly higher standard entropy. It is highlighted that the parameters given in terms of polynomial functions of temperature that were employed so far in 3rd generation models to describe anharmonic contributions in the heat capacity of compounds were not suited to satisfactorily describe the thermodynamic properties of crystalline CaO. It is suggested that this observation can be generalized to most refractory oxides. Alternative terms are proposed in the Gibbs energy function that give more flexibility in fitting the experimental data and lead to more numerically reasonable values for the parameters. The liquid and amorphous CaO phase is described using the two-state model, leading to a significant improvement in the description of its heat capacity. The description of crystalline CaO₂ is also improved as only estimates of the thermodynamic properties of the compound were available in previous modellings of the system. Finally, phase equilibria data on the Ca – CaO liquidus is reviewed, and it is highlighted that slight discrepancies in the relatively low temperature measurements can lead to significantly different descriptions of the liquid phase.

1. Introduction

Discussions at the 1995 Ringberg meeting aimed at improving the current thermodynamic models. On the one hand, it was recommended for crystalline phases to replace the phenomenological polynomial description of the temperature dependence of the heat capacity by an extended Debye or Einstein model [1]. In addition to an improved physical meaning, doing so allows to model the thermodynamic properties of the phases down to 0 K, enabling a better integration of data from first-principles calculations. On the other hand, it was recommended to model the liquid phase using the so called Two-State model [2], in which atoms are either considered to be in an amorphous-like or in a liquid-like state. The motivation behind this change is that using the traditional polynomial description of the temperature dependence, extrapolations beyond the stability range of the phases may lead to spurious predictions, such as artificial phase stability, or the so-called Kauzmann and inverse Kauzmann paradoxes [2]. Following those guidelines, various authors [3-9] are currently working toward the development of the so-called 3rd generation databases.

From the review of the Ca – O system performed by Wriedt [10], the known stable compounds are solid CaO, which is stoichiometric up to at least 1400 K, and solid CaO₂, which is unstable at room temperature and atmospheric pressure. The CaO₄ and CaO₆ compounds might be stable at high oxygen pressures and low temperatures, but their existence was not demonstrated through experiments yet.

Solid CaO, with its common mineral name "lime", is an important compound for many applications. It is the key active component in building materials (lime-silicates and lime-aluminates [11]), in geochemistry and planetology [12], metallurgical slags [13] and glass-forming oxides [14]. It is therefore one of the key constituents in any Calphad based thermodynamic database for oxides such as the FactSage FToxid database [15].

The thermodynamic properties of phases in the Ca – O system were described by various authors [16-18] based on different thermodynamic models and experimental data. Hillert et al. [16] gave a partial description of the system up to CaO using the ionic model for the liquid phase. A more complete description on the whole composition range including the CaO₂ compound was proposed by Lindberg et al. [17]. In this work, the liquid phase was described using the modified quasi-chemical model, but the validity of its description is limited to the partial Ca – CaO system as it was highlighted by Liang et al. [18]. The most recent description of the Ca – O system was provided by Liang et al. [18] based on a remarkably thorough assessment of the existing literature data. The associate solution model was used by the authors to describe the liquid phase in the whole composition range. Compared to the description proposed by Lindberg et al. [17], the Ca – CaO liquidus was reassessed and the melting point of CaO was revised to a value which is almost 400 K higher than some experimental values in the literature based on a recent investigation conducted by Manara et al. [19].

This work aims at improving the thermodynamic description of the Ca – O system, and 3rd generation models are used to describe crystalline CaO, liquid and amorphous CaO as well as of crystalline CaO₂. Thermodynamic data recently obtained by first principles Density Functional Theory (DFT) calculations and molecular dynamics simulations are used to obtain a robust description of the thermodynamic properties of the phases of the system. Compared to previous assessments, the description of the heat capacity and entropy of crystalline and liquid and amorphous CaO is improved as well as the modelled thermodynamic properties of CaO₂ that were based on estimations so far. Regarding the phase equilibria data, the literature on the Ca – CaO liquidus is reviewed, and it is highlighted that slight discrepancies in the relatively low temperature measurements can lead to significantly different descriptions of the liquid phase.

2. Review of the literature data

2.1. Thermodynamic properties of crystalline CaO

Significant discrepancies can be found in the experimental literature data on the standard enthalpy of formation of CaO. Indeed, Gourishankar et al. [20] derived from free-evaporation experiments an enthalpy of -602 kJ.mol^{-1} , which is 33 kJ.mol^{-1} more positive than the values obtained from bomb calorimetry [21] and acid solution calorimetry [22]. After conducting a thorough and critical investigation of the literature data, Liang et al. [23] suggested a value of $-634 \pm 1.5 \text{ kJ.mol}^{-1}$ for the standard enthalpy of formation of CaO. The proposed enthalpy is in perfect agreement with the value of $-634.6 \text{ kJ.mol}^{-1}$ obtained from DFT calculations by Pisch et al. [24]. Therefore, this value is selected in the present modelling.

Regarding the heat capacity and heat content of crystalline CaO, several independent dataset are available in the whole 4 – 3086 K range. The heat capacity data [25-27] in the literature are plotted in Fig. 1, and the available heat content data [28-37] represented in Fig. 2. Although the experimental data are essentially consistent, some discrepancies can be found, leading to different choices in the modelling and impacting the stability of crystalline CaO. Pisch et al. [24] performed phonon calculations, which can be a powerful tool in critically assessing conflicting literature data [38]. Calculations were performed by the authors in the quasi-harmonic approximation using the Strongly Constrained and Appropriately Normed (SCAN) functional [39] and results are also plotted in Fig. 1 and 2. The validity of such ab initio calculations is generally limited in temperature to roughly two third of the melting point of the compound, and the DFT dataset is therefore limited at approximately 2000 K. Below 298.15 K, the phonon calculations were found to be in a better agreement with the measurements from Park et al. [26] compared with the results from Nernst et al. [25] and Gmelin et al. [40]. The latter datasets are therefore not used in the present modelling. The discrepancy stems most likely from the experimental difficulty to obtain pure, dense bulk samples of CaO for the measurement. As an example, one can cite the work from Gmelin [27, 40]. The sample preparation is described in the earlier paper. The CaO sample was prepared by electronic melting at very high temperature followed by a sintering step. The obtained sample is very pure from a chemical point of view, but its density is more than 30% less than the theoretical value. It is obvious that the measurement of thermodynamic properties such as the heat capacity at constant pressure on samples with high porosity is difficult to perform (thermal equilibration in the calorimeter) which increases the uncertainty in the measurement. Consequently, a value of $40.35 \text{ J.mol}^{-1}.\text{K}^{-1}$ is selected in this work for the absolute entropy of CaO, derived from the DFT phonon calculations in the quasi-harmonic approximation, which is slightly higher than the value of $38.21 \text{ J.mol}^{-1}.\text{K}^{-1}$ compiled in the JANAF tables [41]. Above 300 K, the heat content as a function of temperature as derived from the phonon calculations by Pisch et al. [24] were found to be in rather good agreement with most datasets [28, 30-33, 35-37], except the heat content proposed by Roth et al. [29] and Chekhovskoi et al. [34]. Therefore, the latter datasets were not taken into account in the modelling. It is however to be noted that Chekhovskoi et al. [34] are the only experimental data available in the 2000 – 3086 K range, and the trend measured by the authors clearly features a greater increase of heat content above roughly 2600 K. Additional information were provided in this rather high temperature range by Alvares et al. [37] who performed classical molecular dynamics simulations on crystalline CaO. Due to the specific Born-Mayer-Huggins (BMG) potential used by the authors, the molecular dynamics heat contents are shifted in enthalpy compared to the accepted data, and they are therefore not used in the modelling. However, the ab initio data feature a trend similar to that reported by Chekhovskoi et al. [34]. A sudden heat content increase before the melting point is frequently observed in oxides [42]. This trend is known as pre-melting effect and is due to different melting behavior of the anionic and cationic sublattices in the crystal structures of oxides. Therefore, the present modelling aim at reproducing this characteristic trend. To do so, valuable anchor points were provided by Alvares et al [37] who also performed ab initio molecular dynamics using the SCAN interaction functional [39]. Only three data points were calculated this way for crystalline CaO due to the very high computation time required. The data point at 1500 K is in satisfying agreement with the accepted heat content data, supporting the validity of the calculations.

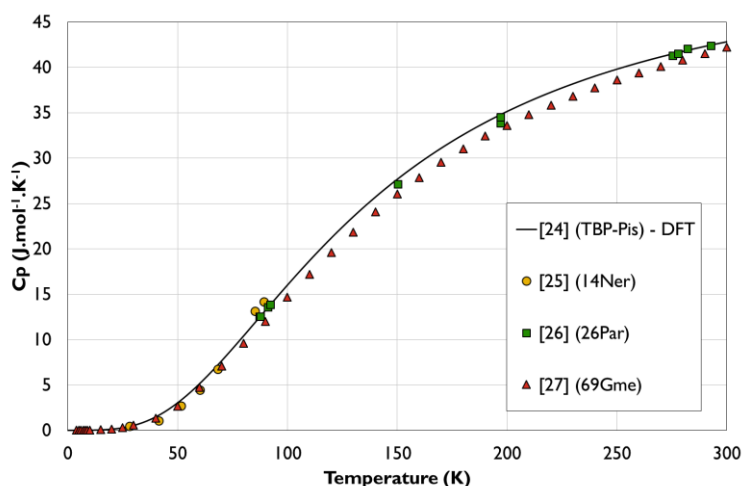


Fig. 1. Literature heat capacity data on crystalline CaO. It is noted that the DFT calculations from Pisch et al. [24] are available up to 2000 K, but the X-axis scale was reduced at 300 K for a better resolution in the comparison of the different datasets.

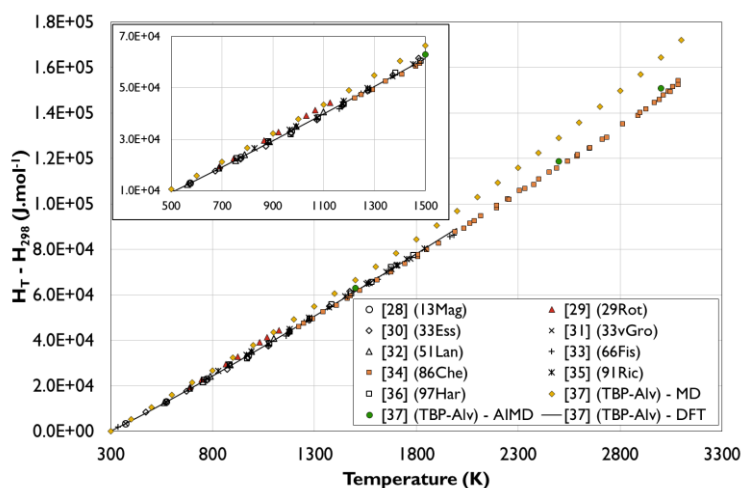


Fig. 2. Literature heat content data on crystalline CaO. Inlet: zoom on the area where the most datasets are available.

2.2. Thermodynamic properties of liquid and amorphous CaO

Regarding the thermodynamic properties of liquid and amorphous CaO, no experimental data could be found in the literature. Indeed, the rather very high melting point of the compound makes experimental work extremely challenging. The heat capacity of the liquid above the melting point was estimated by Gurvich et al. [43] at $84 \pm 10 \text{ J.K}^{-1}.\text{mol}^{-1}$ based on analogy with experimental data on liquid BeO and BaO. Alvares et al. [37] calculated the heat content of liquid CaO in the 2200 – 4000 K range by molecular dynamics simulations. Similarly to the heat content obtained for crystalline CaO, the calculated data are shifted in enthalpy due to the potential used by the authors, and the raw data are therefore discarded. However, as no other experimental information are available, the heat content trend was retained as the original data were converted into heat capacity data where a shift in enthalpy have a less significant impact. The converted data are consistent with the estimations from Gurvich et al. [43] and are accepted in the present assessment. In addition, Alvares et al. [37] calculated the heat content of liquid CaO at 3200 K by ab initio molecular dynamics. A value of 248.2 kJ/mol was obtained with respect to crystalline CaO at 300 K and is selected in the present assessment.

2.3. Data relative to the melting of CaO

The data regarding the melting of CaO were reviewed by Liang et al. [18] and discussed by Manara et al. [19]. Due to very delicate experimental work, conflicting values ranging from 2843 K to 3223 K have been reported in the literature data. It is to be noted that both the measurements and their interpretation are challenging, as it is unsure whether CaO is melting or boiling, if the reaction is congruent or not, and even whether the compound is stoichiometric or not at such high temperatures [10]. Manara et al. [19] conducted a remarkable experimental study of the melting of CaO by quasi-containerless laser heating under different atmospheres. Under an oxidizing environment (air at 0.3 MPa), the authors measured a solidification point at 3222 ± 25 K that they attributed to the congruent melting of CaO due to the seemingly negligible influence of the pressure on the measured value. Under a reducing environment (Ar + 6% H₂ at 0.3 MPa), the authors measured a solidification point at 3192 ± 40 K that they attributed to the three-phase equilibria between a crystalline CaO, a CaO liquid with oxygen defects, and a gas.

Regarding the enthalpy and entropy of fusion of CaO, no experimental data are available. The entropy of fusion was reported in the JANAF tables [41] at $25.06 \text{ J.K}^{-1}.\text{mol}^{-1}$, although it has to be noted that this value is purely estimated. A similar estimation of $25 \pm 5 \text{ J.K}^{-1}.\text{mol}^{-1}$ was made by Gurvich et al. [43] based on the entropy of melting of BeO and other alkaline-earth metal oxides. The corresponding enthalpy of fusion at the selected temperature of 3222 K is calculated at $80 \pm 16 \text{ kJ.mol}^{-1}$. The molecular dynamics simulations conducted by Alvares et al. [37] lead to a very similar enthalpy of fusion of $80.92 \text{ kJ.mol}^{-1}$. Therefore, this value was accepted in the present assessment. It is noted that this enthalpy of fusion is also in a satisfying agreement with the data obtained before and after the melting by ab initio molecular dynamics by Alvares et al. [37] as it will be highlighted when presenting the results of the modelling.

2.4. Thermodynamic properties and thermal stability of CaO₂

Very limited information are available regarding the CaO₂ compound. The calcium peroxide is only stable at rather high oxygen pressures, as the oxygen pressures in equilibrium with both CaO and CaO₂ at room temperature were reported to be about 1 bar [10]. However, there is debate in the literature concerning the stability of this compound under standard conditions. Brosset and Vannerberg [44] tried to synthesize this compound using the standard experimental procedure from the literature. Instead of getting pure CaO₂, they ended up with an oxide-hydroxide compound when carefully analyzing the sample, indicating that the pure oxide compound may be unstable at room temperature. Neither its melting point nor its thermodynamic properties have been measured [10]. This compound is not entered in the JANAF tables [41], and estimations of its thermodynamic properties can be found in [45]. Recently, the thermodynamic properties of CaO₂ have been determined by DFT and phonon calculations by Pisch et al. [24]. Those data are considered as robust supported by the fact that the calculations performed by the authors on crystalline CaO are in very good agreement with the experimental literature.

2.5. Data relative to the Ca – CaO Liquidus

Five dataset related to the Ca – CaO liquidus are available in the literature. They were obtained in three independent investigations, and lead to four conflicting trends. To begin with, the experimental work will be reviewed. In a second time, the dataset will be presented and compared with previous modelling of the system, and the agreement between the different sources as well as the data selection will be discussed. In the experimental literature, the liquidus was always expressed in mole percent of CaO. In this work, the data were converted into atomic percent of oxygen using the following equation:

$$x_o = \frac{x_{CaO}}{1 + x_{CaO}} \quad (1)$$

First of all, the solubility limit of CaO in liquid Ca was estimated by Bevan et al. [46]. The authors performed a visual comparison of the size of CaO pellets before and after the thermal treatment of 20 mole percent of CaO in liquid Ca at 1523 K. On this basis, a solubility of $14.2 \pm 1.5 \text{ at.}\% \text{O}$ ($16.5 \pm 1.5 \text{ mol.}\% \text{CaO}$) was proposed.

Then, the Ca – CaO Liquidus was determined in the 1233 – 1705 K range by both chemical and differential thermal analyses by Fischbach [47]. The author used 99% pure Ca, that was stored and handled in protective atmosphere. Regarding CaO, it was stated that its purity was controlled “very carefully”, but no quantitative information are given. Unfortunately, no further experimental details are available as only experimental work performed on Ca – CaF₂ and Ca – CaCl₂ slags were described by the author, and it is uncertain that the followed procedure was the same. It is however noted that the experimental work performed by Fischbach [47] on Ca – CaF₂ and Ca – CaCl₂ slags was meticulous, and that a special care was given by the author on having an efficient quenching procedure so that no segregation effects would occur during cooling.

More recently, Zaitsev et al. [48, 49] measured the activity of Ca in the liquid in two-phase equilibria with CaO in the 1165 – 1723 K range, and the authors also stated that they measured the solubility limit of CaO in liquid Ca in the same temperature range. The materials used by the authors are 99.9 wt.% pure Ca, and CaO of unknown purity obtained by thermal decomposition CaCO₃. The samples were sealed in iron or molybdenum vessels that were carefully degassed prior to the experiments. Regarding the activity measurements, a static method was used by the authors [49] as the partial pressure of Ca in the investigated temperature range is too high for the Knudsen technique. The experimental assembly consisted in two dismountable chambers connected so that the gas could flow between them but not the condensed phases. The equilibrium Ca partial pressure on top of saturated Ca – CaO samples was determined from the volume of the top unfilled chamber and the amount of evaporated calcium. The latter was determined by chemical analysis from the condensate on the walls of the chamber in question. In order to verify the validity of their experimental procedure, the authors measured the vapour pressure of pure Ca from 1473 to 1673 K, and they found those measurements to be in good agreement with the accepted literature data. The authors derived activity data from their measurements using up-to-date data on pure Ca as it was carefully checked by Liang et al. [18]. A source of error may come from the presence of additional species in the gas phase such as CaO or O₂ that were not considered by the authors. Therefore, thermodynamic calculations were performed using the Ca – O description proposed by Liang et al. [18], and Ca was found to be the only significant specie present in the gas in this temperature and composition range. Similar results were obtained using the database resulting from this work as Ca and Ca₂ are calculated to be the largely predominant species in this temperature and composition range. Regarding the solubility measurements, Zaitsev et al. [49] reported that equilibrated Ca – CaO samples were quenched, and that the calcium content in the samples was determined by chemical analysis by the induction-bound plasma technique. It was noted by the authors that when the melts were unsaturated, the determined calcium concentration was in good agreement with the initial composition. In their literature review, Liang et al. [18] discarded those solubility data from Zaitsev et al. [49] because the assessors reached the conclusion that the authors did not actually performed the measurements. The main reason behind this is that the solubility data proposed by Zaitsev et al. [49] appear to be smoothed and do not feature the expected experimental scatter. This is even more striking when looking at the Ca – CaO partial phase diagram proposed by Zaitsev et al. [49]. In this figure, the authors only represented their proposed solubility data featuring the best agreement, discarding 5 data points over 19 in the process. As the authors mentioned that they performed measurements on unsaturated samples, one can wonder if those 5 data points are part of it or not as no comments can be found on this matter in the discussion. It seems that the authors did not discard the activity measurements obtained at the corresponding temperatures, therefore it is assumed that this choice was made to make the proposed phase diagram look better.

The reported data [46, 47, 49] on the solubility limit of CaO in liquid Ca are plotted along with the results from previous modellings of the Ca – O system [17, 18] in Fig. 3. In order to evaluate the overall agreement between the activity measurements from Zaitsev et al. [49] and the literature solubility data [46, 47, 49], the liquidus modelled by Liang et al. [18] when only fitting those data is also presented in Fig. 3. Several important observations can be made from this plot.

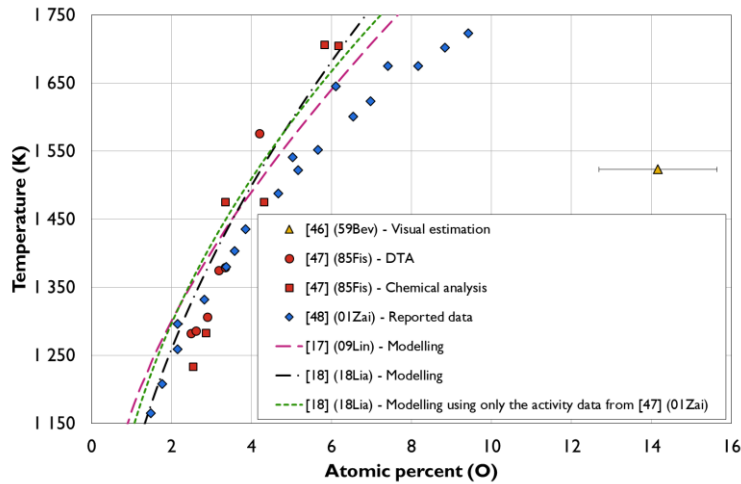


Fig. 3. Reported literature data on the Ca – CaO liquidus along with the results from previous modellings of the system. The black dash-dotted line is the liquidus accepted by Liang et al. [23] whereas the green densely dashed line is the liquidus obtained by the same authors when fitting only the activity data measured by Zaitsev et al. [49].

First of all, it is noted that the data point estimated by Bevan et al. [46] is very far off from any other literature data. The visual determination performed by the authors may give a first estimate but is obviously not reliable, and this data point is therefore discarded.

Then, a very good agreement was obtained between the dataset measured by Fischbach [47] with both chemical and differential thermal analyses. This supports the validity of the experimental procedure followed by the author.

It is interesting to focus next on the agreement between the solubility data from Fischbach [47] and the activity measurements from Zaitsev et al. [49], which can be roughly evaluated in Fig. 3 by comparing the former data with the liquidus proposed by Liang et al. [18] when only fitting the latter data. Although a reasonable agreement is obtained in the 1450 – 1750 K range, both liquidus feature conflicting trends. If the disagreement may not be significant in this temperature range, this implies different choices in the temperature dependency of the interactions of the constituents in the liquid phase that result in sensibly different descriptions at higher temperatures as it will be highlighted later in the discussion.

Finally, it is highlighted in Fig. 3 that the solubility data reported by Zaitsev et al. [49] deviate significantly from the other dataset with increasing temperature. If those are not actual experimental measurements as suggested by Liang et al. [18], this disagreement would come from the derivation performed by the authors to obtain those data. If those are actual experimental measurements, it is likely that the solubility limit of CaO in saturated liquid Ca was overestimated by taking undissolved CaO particles during the sampling, as it seems that no special care was taken by the authors on this matter. In either case, this dataset is considered doubtful and is discarded in the present assessment.

In conclusion, after discarding the estimated data from Bevan et al. [46] and the reported solubility data from Zaitsev et al. [49], the two remaining dataset relative to the Ca – CaO liquidus are the activity measurements from Zaitsev et al. [49] and the solubility data from Fischbach [47]. Although given the experimental uncertainties both dataset are in an acceptable agreement, they feature two conflicting trends that can lead to significant differences in the modelling at higher temperatures. In this work, the direct solubility measurements from Fischbach [47] are preferred as activity measurements represent more delicate experimental work. This choice is also supported by the fact Fischbach [47] obtained consistent datasets using two different experimental procedure. Nonetheless, as this choice is not straightforward, the activity measurements from Zaitsev et al. [49] will also be fitted in a separate attempt, and the results obtained in both cases will be compared and discussed.

2.6. Invariant Ca/CaO eutectic reaction

Bevan et al. [46] measured by thermal analysis the eutectic between β -Ca and CaO using sealed iron containers. The authors measured the melting point of β -Ca at 1110 ± 1 K, which is 5 K lower than the accepted value of 1115 K. The eutectic temperature was measured at 1107 ± 1.5 K on the basis of three different compositions. Wriedt [10] retained the measured difference of 3 K between both measurements and suggested the eutectic temperature of 1112 K based on the accepted melting point of β -Ca. Doubts have been raised in the literature [18, 47] regarding the purity of the materials used by Bevan et al. [46]. Indeed, no information are given by the latter authors [46] on this matter, and the relatively low melting point of β -Ca obtained by the authors suggests purity issues. Plus, the solubility of CaO in liquid Ca that the authors [46] visually estimated to be 14.2 ± 1.5 at.%O (16.5 ± 1.5 mol.%CaO) at 1523 K is roughly 3 times higher than the experimental measurements from Fischbach [47] as shown in Fig. 3. Therefore, the eutectic temperature measured by Bevan et al. [46] is considered doubtful in the present assessment.

Nonetheless, the activity measurements performed by Zaitsev et al. [49] and the Ca – CaO solubility data obtained by Fischbach [47] suggest that the invariant point composition is lower than roughly 1.5 at.%O, which is consistent with the fact that the eutectic temperature should be rather close to the melting point of pure Ca. Bevan and Richardson [46] estimated the eutectic liquid oxygen content at 0.3 "mole per cent.", but a composition of 1.5 mol% CaO was drawn on the corresponding figure which is most confusing.

In conclusion, the temperature of the eutectic involving β -Ca and CaO is, although uncertain, likely to be located between 1105 K and 1114 K.

3. Thermodynamic modelling and optimization procedure

3.1. Model for crystalline CaO and CaO₂

Discussions at the 1995 Ringberg meeting [1] aimed at finding a universal model for the thermodynamic properties of crystalline phases that could give a satisfactorily fit of the data from very low to very high temperatures while carrying physical meaning and being easy to implement in thermodynamic databases. It was recommended as a compromise to describe the heat capacity of compounds either using an Einstein or a Debye model with a constant Debye or Einstein temperature and additional terms given in terms of polynomial functions of temperature to account for the rise of anharmonic contributions at higher temperatures. Although the Debye model gives better results in describing the heat capacity at low temperature, the Einstein model was preferred by Chen and Sundman [9] and following modelers [3-7] as it is easier to implement. The heat capacity of a crystalline phases can then be expressed, excluding any potential magnetic transformations, as [9]:

$$C_p = 3R \left(\frac{\theta_E}{T} \right)^2 \frac{\exp\left(\frac{\theta_E}{T}\right)}{\left(\exp\left(\frac{\theta_E}{T}\right) - 1\right)^2} + aT + bT^4 \quad (2)$$

where θ_E is the Einstein temperature, and where the aT term is here to account for non-thermodynamic information such as the electron density of states at the Fermi level and the bT^4 term for the high-order anharmonic lattice vibrations. It is noted that when modelling a compound, the Einstein contribution of Eq. 2 should be multiplied by the phase stoichiometry. It is underlined for the upcoming discussion that it was initially recommended at the Ringberg workshop [1] to have a bT^2 term instead of a bT^4 term, and the reason why Chen and Sundman [9] changed it was for the model to be able to fit a wider spectrum of phases while also resulting in more reasonable numerical values for the parameter a .

Above the melting point, in order to avoid absurd extrapolation of the metastable crystalline solid at very high temperatures that may lead to its re-stabilization, it was recommended by Chen and Sundman [9] to make the heat capacity of the solid tends to the heat capacity of the liquid phase at an arbitrary chosen high temperature. The expression recommended by the authors to enable this while ensuring the continuity of the thermodynamic properties and their derivative at the junction is the following:

$$C_p = 3R \left(\frac{\theta_E}{T} \right)^2 \frac{\exp\left(\frac{\theta_E}{T}\right)}{\left(\exp\left(\frac{\theta_E}{T}\right) - 1\right)^2} + a' + b'T^{-6} + c'T^{-12} \quad (3)$$

The model was successfully used by various authors [5-7] to describe the thermodynamic properties of Mn, Co and Pb. However, a satisfying fit could not be obtained using a single characteristic Einstein temperature for C [4] and Sn [3]. Using multiple Einstein temperatures, Eq. 2 is modified as following:

$$C_p = 3R \sum_i \alpha_i \left(\frac{\theta_i}{T} \right)^2 \frac{\exp\left(\frac{\theta_i}{T}\right)}{\left(\exp\left(\frac{\theta_i}{T}\right) - 1\right)^2} + aT + bT^4 \quad (4)$$

where the sum of the α_i coefficients have to be roughly equal to the phase stoichiometry.

In the present work, multiple Einstein temperatures had also to be used to give a satisfactory description of calcium oxides as it will be highlighted later in the discussion.

In addition, the heat capacity of CaO could not be satisfactorily modeled using the additional aT and bT^4 terms presented in Eq. 4. The reason is that CaO features a sudden increase in heat capacity from the rather very high temperature of roughly 2600 K, which those terms can simply not reproduce. It is reminded here that an increase of heat capacity before melting is a common feature for oxides as briefly discussed in section 2.1. A better fit could be obtain either by using $aT + bT^{12}$ terms, or $aT + bT^6 + cT^7$ terms instead of the recommended $aT + bT^4$ terms. However, finding the adequate polynomial function of the temperature was proven not to be straightforward. In addition, when using high power polynomial terms, the corresponding parameters may have unreasonable numerical values, such as roughly 10^{-40} for the bT^{12} term in the present case of modelling CaO. This may causes issues for the calculations software, as the mentioned b parameter was for instance rounded to 0 by the Thermocalc software [50] when entered as a function in a database. In conclusion, using a polynomial function of the temperature does not seem adapted to model the anharmonic contribution in the heat capacity of refractory oxides. Therefore, in this work, the following expression was used to describe the heat capacity of crystalline phases below their melting point:

$$C_p = 3R \sum_i \alpha_i \left(\frac{\theta_i}{T} \right)^2 \frac{\exp\left(\frac{\theta_i}{T}\right)}{\left(\exp\left(\frac{\theta_i}{T}\right) - 1\right)^2} + aT + T \exp(b + cT) \quad (5)$$

where the b parameter is only a horizontal shift of the heat capacity increase, and the c parameter influence on its shape. The proposed $T \exp(b+cT)$ term was proven to be much more flexible in describing very high temperature heat capacity trends compared with powers of T , as it can fit very sharp increases and well as more monotonous trends. In addition, the quality of fit was also better, as only optimized powers of T terms in the form of $bT^d + cT^e$ could have given similar results. Finally, the numerical values of the related parameters are more reasonable as it will be highlighted when presenting the optimized parameters. It has to be noted, however, that this exponential term is very sensitive to the parameters value, and without a proper starting point the optimization software might fail to find a solution. Indeed, depending on the initial input for the b and c parameters, the exponential term might be unreasonably large or small. In order to find a good starting point easily, it is suggested to begin with fitting a numerically reasonable heat capacity contribution (e.g. $10 \text{ J}\cdot\text{mol}^{-1}\cdot\text{K}^{-1}$) at the melting point with this exponential term, that is to say:

$$T_{fus} \exp(b + cT_{fus}) = C_{p\text{arbitrary}} \Leftrightarrow b + cT_{fus} = \ln\left(C_{p\text{arbitrary}}\right) - \ln(T_{fus}) \quad (6)$$

with T_{fus} the melting point, and $C_{p\text{arbitrary}}$ a numerically reasonable heat capacity value. From this point, by taking arbitrary equivalent contributions of the b and c parameters at the melting point, that is to say $c = b/T_{fus}$, the following starting values are obtained :

$$b = cT_{fus} = \frac{\ln(C_{p_{arbitrary}}) - \ln(T_{fus})}{2} \quad (7)$$

In the particular case of CaO, by taking $C_{p_{arbitrary}}$ equal to $10 \text{ J.mol}^{-1}.\text{K}^{-1}$ and a melting point of 3222 K, one obtain a starting value for the optimization of -3 for b and -9.10^{-4} for c.

By integration Eq. 5, the following Gibbs energy expression is found for the solid below its melting point:

$$G = E_0 + \frac{3}{2}R \sum_i \alpha_i \theta_i + 3RT \sum_i \alpha_i \ln\left(1 - \exp\left(-\frac{\theta_i}{T}\right)\right) - \frac{a}{2}T^2 - \frac{\exp(b + cT)}{c^2} \quad (8)$$

To avoid unrealistic extrapolation of CaO above its melting point, it was attempted to use Eq (2) as proposed by Chen and Sundman [9]. However, as the heat capacity increase is rather steep and due to the very high melting point temperature of 3222 K, to have a continuous heat capacity derivative at the junction resulted in the heat capacity of the solid to be much higher than the heat capacity of the liquid at higher temperatures as the $b'T^{-6}$ and $c'T^{-12}$ terms were not enough to dampen it. Indeed, the higher the junction temperature, the less stiff is the heat capacity curvature using negative powers of T terms. In fact, no viable solutions were found using any combination of negative powers of T, therefore the expression was once again adapted as following:

$$C_p = A - \frac{T}{(B + CT)^3} \quad (9)$$

First of all, at very high temperatures the Einstein model tends to the constant value of $3R$ per atoms which can be redundant with the parameter a' of Eq. 3, therefore it was removed from the expression to keep it as simple as possible. Then, a $T/(B+CT)^3$ term was used, where the B parameter allows to shift the heat capacity dampening along the temperature axis, and the C parameter enable to fit the required curvature at the junction. The reason the denominator is up to the power 3 is to avoid having any logarithmic terms appearing when integrating the heat capacity expression to obtain S, H and G, as negative values would then result in errors in the calculations. The A parameter can be directly set at the desired high temperature heat capacity constant value, and the B and C parameters are optimized using the conditions of continuity of the heat capacity and its derivative at the junction.

By integration Eq. 9, the following Gibbs energy expression is found for the solid above its melting point:

$$G = H' - S'T + AT(1 - \ln(T)) + \frac{1}{2C^2(B + CT)} \quad (10)$$

Where parameters S' and H' are optimized using the conditions of continuity of the entropy and the enthalpy at the junction.

3.2. Model for liquid and amorphous CaO

The liquid and amorphous phases were described using the two-state model discussed during the 1995 Ringberg meeting [2] and based on previous works from Ågren [51]. This model considers that atoms or molecules in the liquid phase are either in the amorphous-like state, featuring only vibrational degrees of freedom, or in the liquid-like state, with translational degrees of freedom. The general expression for the Gibbs energy of the amorphous-liquid phase is then given as following:

$$G^{liq-am} = G^{am} - RT \ln\left(1 + \exp\left(-\frac{\Delta G_d}{RT}\right)\right) \quad (11)$$

Due to a lack of information on the thermodynamic properties of amorphous CaO, its Gibbs energy can be taken in first approximation as [2]:

$$G^{am} = G^{cryst} + A + BT \quad (12)$$

First of all, it is important to note that, as suggested by Chen and Sundman [9], the term accounting for the high-order anharmonic contributions in the Gibbs energy of the crystalline state, in the form of an exponential in this work, was excluded of the description of the amorphous phase. Then, Ågren and co-workers [2] pointed out that for the amorphous state to obey the third law of thermodynamics, B should be taken equal to 0. In practice, this choice was widely made in the literature [4, 5, 7-9]. Whether glasses such as CaO should have a non-zero residual entropy at the zero absolute temperature raises deep questions on our understanding of such materials, as it is from instance showcased in the eloquent discussion of Schmelzer et al. [52]. This work does not intend to take position in a theoretical point of view on the matter, but the influence of the residual entropy at 0 K on the modelled thermodynamic properties of CaO will be presented and discussed.

Finally, the ΔG_d term in Eq. 11 stand for the Gibbs energy difference between the liquid-like and the amorphous-like atoms, and can be expressed in a classical CALPHAD expansion [2] :

$$\Delta G_d = A + BT + CT \ln(T) + \dots \quad (13)$$

As a starting point, it is recommended in the literature to either set B to the value of the gas constant R [2, 7, 51] or to the entropy of fusion [5, 8, 9], and the parameter A to the enthalpy of fusion [5]. The parameter C may be optimized in a second time if data are available and are not satisfactorily fitted by using only A and B [5]. It is however noted that, because the heat capacity of the amorphous CaO was taken equal to the one the crystalline phase excluding the terms accounting for the high-order anharmonic contributions, the heat capacity of the liquid phase would be lower than the one of the crystalline phase after the melting point without using the parameter C. This parameter is therefore needed here, and as a starting point one can simply take the difference in heat capacity between the modelled amorphous phase and the liquid phase at the melting point. Starting value for the parameters B and A can be found afterwards under the rough approximation that 60% of the atoms are in the liquid-like state at the melting point by using the parameter C, the modelled properties of the amorphous and of the crystalline phases, and the entropy and enthalpy of fusion. It is further noted that using the parameter C that should be negative, the parameter B may be positive, which would mean that the entropy of the amorphous phase is higher than the one of the liquid phase in the very low temperature range. While this is unphysical, it is directly linked to the fact the Gibbs energy difference between the liquid-like and the amorphous-like atoms is expressed in a 2nd generation CALPHAD expression, which is typically not valid below 298.15 K. Finally, it is also noted here that the parameter A should always be positive so that the atoms start in the amorphous-like state at low temperature.

3.3. Model for the Ca – O binary liquid phase

Liang et al. [18] highlighted that in the Ca – O system the liquid model need to be able to accounts for the strong short-range ordering, significant even at low oxygen content of only a few at.%. In this work, the liquid phase is described with a three species associate model [53, 54], where CaO was chosen as the intermediate associate. The Gibbs energy of the liquid phase is presented in the following equation:

$$G_m^{liq} = \sum_k x_k G_k^{liq} + RT \sum_k x_k \ln(x_k) + \sum_i \sum_j x_i x_j {}^0L_{i,j}^{liq} \quad (14)$$

where i, j and k are the species Ca, CaO and O, x_i , x_j and x_k their molar fraction, G_k^{liq} their molar Gibbs energy in the liquid phase, and ${}^0L_{i,j}^{liq}$ the zero-order Redlich-kister binary interaction parameter between the species i and j in the liquid phase. The temperature dependency of ${}^0L_{i,j}^{liq}$ is taken into account according to the following equation:

$${}^0L_{i,j}^{liq} = {}^0a_{i,j}^{liq} + {}^0b_{i,j}^{liq} T \quad (15)$$

where ${}^0a_{i,j}^{liq}$ and ${}^0b_{i,j}^{liq}$ are the parameters of the optimization. Due to the limited range of existence of the available literature data, the liquid solution was kept regular, meaning that no further composition dependency than the $x_i x_j$ multiplicative factor was introduced in the binary interaction parameters.

3.4. Selection of the unary data and description of the gas phase

The description of $O_{2(g)}$ and of liquid and solid Ca are taken from the SGTE unary database [55] in its version 5.1. The description for the gas phase is taken from the SGTE substance database [56] and is constituted of species Ca, Ca_2 , O, O_2 , O_3 and CaO. Its validity is limited at a minimum temperature of 298.15 K, yet calculations had to be performed below this lower limit as the CaO_2 phase was found to decompose at lower temperatures to form crystalline CaO and a gas. In the oxygen-rich region where the decomposition occurs, O_2 is the predominant specie in the gas phase at 298.15 K as the occupancy of any other constituents is calculated to be lower than 10^{-29} . Therefore, the contribution of the Ca, Ca_2 , O, O_3 and CaO species in the Gibbs energy of the gas phase is negligible in the region of interest below ambient temperature. As a result, only the description of O_2 had to be extended down to 100 K. In the JANAF tables [41], the heat capacity of $O_{2(g)}$ is reported to be constant below 298.15 K, as a difference of less than $0.1 \text{ J}\cdot\text{K}^{-1}\cdot\text{mol}^{-1}$ can be found from this temperature to 100 K. The Gibbs energy of O_2 in the gas phase was therefore modelled using a three parameters CALPHAD expression in the form of $A+BT+CT\ln(T)$. The A, B and C parameters were computed using the conditions of continuity of the thermodynamic properties of $O_{2(g)}$ at the junction temperature of 298.15 K.

3.5. Data selection and optimization procedure

The optimization was performed using the Thermocalc software [50].

First of all, crystalline CaO was modelled. To begin with, the heat capacity of the phase was described up to the compound's selected melting point of 3222 K using the DFT data from Alvares et al. [37] up to 1700 K and the heat content data obtained by the same authors by ab initio molecular dynamics. The reason the DFT heat capacity from 1700 to 2000 K was not taken into account is that the calculations are less reliable when approaching roughly two-thirds of the melting point, and the heat capacity slope started to dampen slightly from this point. In order to fit satisfactorily the steeper heat content increase from roughly 2600 K observed both experimentally [34] and in molecular dynamics simulations [37], the exponential term proposed in Eq. 5. had to be used as discussed in the corresponding section. At the melting point, an arbitrary heat capacity value of $78 \text{ J}\cdot\text{mol}^{-1}\cdot\text{K}^{-1}$, corresponding to roughly 95% of the liquid heat capacity at this temperature, was also selected. The reason behind this choice is that the greater increase in heat content from 2600 K can quickly lead to a very high and unreasonable heat capacity value at the melting point. This artificial anchor point allowed to avoid this while still enabling a very satisfying fit of the selected heat content data and trend. During this whole process, a higher weight was assigned to the selected standard entropy of $40.35 \text{ J}\cdot\text{mol}^{-1}\cdot\text{K}^{-1}$. The number of Einstein temperature needed to obtain a satisfactory fit of the selected data was chosen by trial and error as presented in Fig. 4. When using a single Einstein temperature, the lower temperature heat capacity could not be fitted satisfactorily. This is a known drawback of the model, yet the present description of CaO would be easier to implement in higher order systems and databases using a single Einstein temperature. Therefore, it was attempted to propose a description of the phase using a single Einstein temperature and valid only from 298.15 K nonetheless. However, in order to fit the standard entropy with a single Einstein temperature, the heat capacity value and trend at the corresponding temperature of 298.15 K have to vary significantly from the selected data. Therefore the term "aT", originally dedicated to account for non-thermodynamic information, has to be used to make up for it. As a result, a rather poor fit of the data was obtained on the whole temperature range as it is highlighted on Fig. 4. Using an extra T^3 term in the Gibbs energy of CaO was attempted, but doing so the improvement in the 300 – 2000 K temperature range was made at the expense of the quality of the fit at higher temperatures. Finally, and in order to be able to propose a fit using only a single Einstein temperature, a "BT" term was added in Eq. 8. This term comes from the 2nd generation CALPHAD descriptions and its use lead to a constant shift in the entropy of the phase with respect to temperature. In the present case, this enabled the standard entropy of the phase could be fitted while also having reasonable value and trend for the heat capacity at 298.15 K. As a result, the fit of the data was acceptable above this temperature as it can be seen on Fig. 4. If this solution is proposed as an alternative in this work, it is partly in contradiction with the purpose of the 3rd generation databases, which is to improve the physical meaning of the models and to fit the thermodynamic properties of the phases down to 0 K. It is therefore concluded that multiple Einstein temperatures are needed to give a satisfactory 3rd generation description of CaO. Using two Einstein temperatures according to Eq. 8, the fit is much more satisfying, but it is

still difficult to fit the data in the 1 – 200 K range. This slightly impact the quality of the fit up to 400 K as it can be seen on Fig. 4. Therefore, 3 Einstein temperatures were used to model the heat capacity of crystalline CaO.

In a final stage, the E_0 parameter of Eq. 8 was optimized using the enthalpy of formation calculated by DFT by Pisch et al. [24].

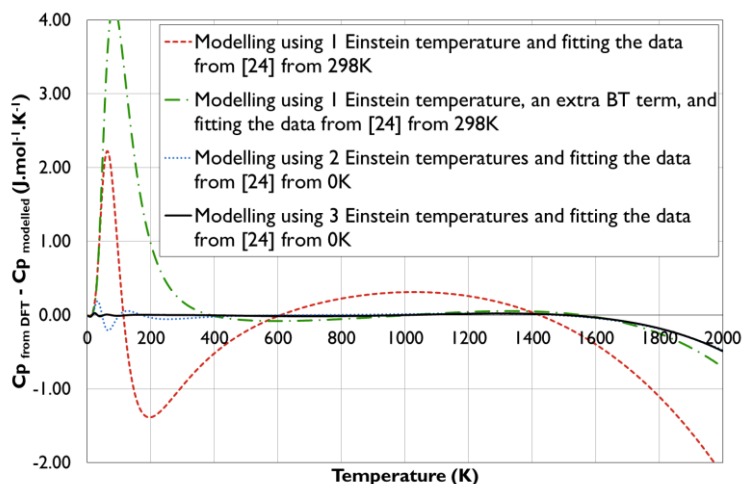


Fig. 4. Difference between the modelled and the heat capacity data of CaO selected from Pisch et al. [24] in the 0 – 2000 K range when using 1, 2 and 3 Einstein temperatures. It is noted that using a single Einstein temperature the data were fitted from 298.15 K in order to try to improve the description at higher temperatures. It is also reminded that the deviation from the selected DFT heat capacity data above 1600 K is made by choice as discussed in the corresponding paragraph.

Then, the heat capacity of crystalline CaO was dampened above the selected melting point of 3222 K in order to avoid unrealistic extrapolation at very high temperature. In order to obtain continuous functions at the junction for the heat capacity and its derivative, the $T/(B+CT)^3$ term proposed in Eq. 9 had to be used instead of the traditional negative powers of T as discussed in the corresponding section. The continuity of the entropy and enthalpy was ensured afterwards by optimizing the H' and S' parameters of Eq. 10.

In a third stage, the liquid and amorphous CaO phase was modelled. Regarding the heat capacity of amorphous CaO, the same description as for crystalline CaO was selected, except for the exponential term proposed in Eq. 5 which was not used. The influence of having a non-zero residual entropy was investigated by fitting the B parameter of Eq. 12 to an arbitrary residual entropy of $3 \text{ J.mol}^{-1}.\text{K}^{-1}$ and the result will be discussed afterwards. In the description of amorphous CaO accepted in this work, the parameter B was kept equal to zero. The parameter A of Eq. 12 was optimized along with the parameters A, B and C of Eq. 13 using the liquid heat content data obtained by molecular dynamics by Alvares et al. [37] and converted in heat capacity, the heat content data point at 3200 K obtained by the same authors by ab initio molecular dynamics, the melting point of 3222 K measured by Manara et al. [19], the enthalpy of fusion of $80.92 \text{ kJ.mol}^{-1}$ calculated by Alvares et al. [37] and the corresponding entropy of fusion of $25.12 \text{ J.mol}^{-1}.\text{K}^{-1}$. A higher weight was assigned to the data relative to the melting of CaO in this process.

In a fourth step, thermodynamic properties of CaO_2 were described. The heat capacity of the compound was modelled using Eq. 5 based on the DFT calculations from Pisch et al. [24] up to 300 K. As the thermal stability of CaO_2 is very limited, one can expect negligible anharmonic contributions in the heat capacity of the compound. Therefore, it was attempted to fit the selected heat capacity data only using the Einstein contribution and without adding extra terms. As for CaO, a higher weight was assigned to the standard entropy during the optimization process. In doing so, a very satisfying result was obtained using 3 Einstein temperatures. Using a single Einstein temperature, only the standard entropy could be fitted as for CaO. Because the CaO_2 compound is not stable above room temperature under 1 bar, a special emphasis should be placed on fitting the low temperature heat capacity of the phase. It was therefore not attempted to provide a description of the phase based

on a single Einstein temperature and valid only above 298.15 K as for CaO. The heat capacity of CaO₂ was described using 3 Einstein temperatures and no extra terms. As a result, it is noted that the modelled heat capacity of the phase tend to the constant value of 3R per atoms at higher temperature. The E₀ parameter of Eq. 8 was optimized afterwards using the enthalpy of formation calculated by DFT by Pisch et al. [24].

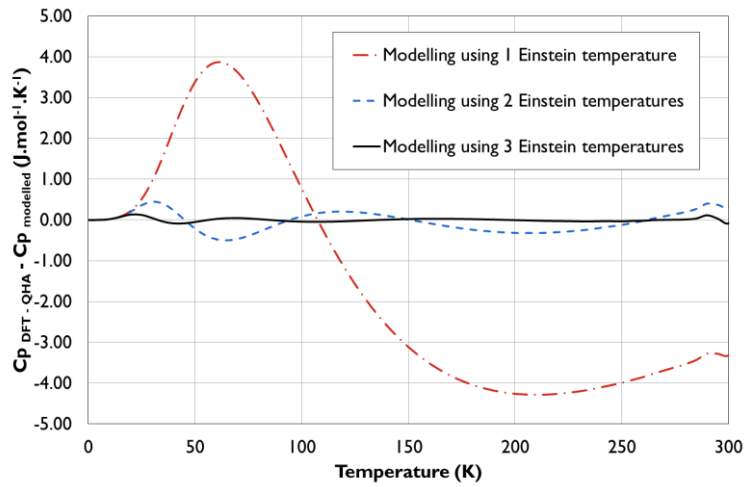


Fig. 5. Difference between the modelled and the selected heat capacity data of CaO₂ in the 0 – 300 K range when using 1, 2 and 3 Einstein temperatures

Finally, the Liquid phase was described using the associate model and is constituted of the Ca, CaO and O species. The Gibbs energy of the Liquid phase was presented in Eq. 14, and binary interaction parameters between the species are described according to Eq. 15. No interaction parameters were modelled between Ca and O. To do so would be meaningless as both species are never present simultaneously in significant amounts. Regarding the interaction between CaO and O, an arbitrary value of +30 was selected for the parameter ${}^0b_{\text{CaO},\text{O}}^{\text{liq}}$ as taken from the work of Liang et al. [18]. This parameter enabled a more satisfactory fit of the observations from Manara et al. [19] as it will be discussed in more details when presenting the modelling results. Finally, regarding the interaction between Ca and CaO, two different sets of parameters were obtained using either the solubility measurements from Fischbach [47] or the activity data from Zaitsev et al. [49]. As it was discussed in the literature review, the accepted set of parameter in this works is the one that lead to a good fit of the solubility measurements from Fischbach [47].

The thermodynamic parameters describing the Gibbs energy of crystalline CaO and CaO₂ were rounded in a way that the thermodynamic properties of those compounds would not vary by more than roughly 10⁻⁰⁵ percent of the fitted values. Regarding the liquid and amorphous CaO phase, the parameters were rounded so that the maximum in the modelled heat capacity would not vary by more than roughly 10⁻⁰⁵ percent. Finally, regarding the interaction parameters in the liquid phase, the proposed parameters are more rounded than the ones mentioned above as the available experimental data are more scarce and uncertain.

3.6. Thermodynamic parameters

The parameters obtained in this modelling are presented in Table 1. In this work, the constant R was taken equal to 8.31446 J.K⁻¹.mol⁻¹ in accordance with the 2018 CODATA recommended values.

Table 1 – Thermodynamic parameters determined in this work in the modelling of the Ca – O system

Gibbs energy of CaO (crystalline) below its melting point ($0 < T < 3222$): $(Ca)_1(O)_1$ – extended Einstein model, according to Eq. 8										
$G_{(Ca)_1(O)_1}^{cryst} = E_0 + \frac{3}{2}R \sum \alpha_i \theta_i + 3RT \sum \alpha_i \ln \left(1 - \exp \left(-\frac{\theta_i}{T} \right) \right) - \frac{a}{2}T^2 - \frac{\exp(b + cT)}{c^2}$										
E_0	α_1	θ_1	α_2	θ_2	α_3	θ_3	a	b	c	$\Sigma \alpha_i$
-652134.4	1.142993	369.447	0.62542	601.229	0.218718	188.291	0.00364916	-15.0586	0.00304142	1.987
Gibbs energy of CaO (crystalline) above its melting point ($3222 < T < 6000$): $(Ca)_1(O)_1$ – according to Eq. 10										
$G_{(Ca)_1(O)_1}^{cryst} = H' - S'T + AT(1 - \ln(T)) + \frac{1}{2C^2(B + CT)}$										
H'		S'		A			B		C	
-731248.3		-492.1078		81.5229			-191.395		0.06241502	
Gibbs energy of CaO (amorphous) ($0 < T < 6000$): $(CaO)_1$ – according to Eq. 12										
$G_{(CaO)_1}^{am} = E_0' + BT + \frac{3}{2}R \sum \alpha_i \theta_i + 3RT \sum \alpha_i \ln \left(1 - \exp \left(-\frac{\theta_i}{T} \right) \right) - \frac{a}{2}T^2$										
E_0'	B	α_1	θ_1	α_2	θ_2	α_3	θ_3	a	Note	
-618466.5	-	1.142993	369.447	0.62542	601.229	0.218718	188.291	0.00364916	Accepted	
-614661.3	3.0	1.142993	369.447	0.62542	601.229	0.218718	188.291	0.00364916	<i>Alternative</i>	
Gibbs energy of CaO (liquid-amorphous) ($0 < T < 6000$): $(CaO)_1$ – according to Eq. 11 and 13										
$G_{(CaO)_1}^{liq-am} = G_{(CaO)_1}^{am} - RT \ln \left(1 + \exp \left(-\frac{\Delta G_d}{RT} \right) \right)$ with $\Delta G_d = A + BT + CT \ln(T)$										
A		B		C			Note			
31233.8		85.5245		-12.76672			Using the accepted description of amorphous CaO			
38814.6		71.14105		-10.95002			<i>Using the alternative description of amorphous CaO</i>			
Gibbs energy of CaO ₂ (crystalline) ($0 < T < 6000$): $(Ca)_1(O)_2$ – according to Eq. 8										
$G_{(Ca)_1(O)_2}^{cryst} = E_0 + \frac{3}{2}R \sum \alpha_i \theta_i + 3RT \sum \alpha_i \ln \left(1 - \exp \left(-\frac{\theta_i}{T} \right) \right) - \frac{a}{2}T^2 - \frac{\exp(b + cT)}{c^2}$										
E_0	α_1	θ_1	α_2	θ_2	α_3	θ_3	a	b	c	$\Sigma \alpha_i$
-676359.7	2.04814	398.195	0.45973	184.418	0.56518	954.326	-	-	-	3.073
Interaction parameter between the CaO and O species in the liquid phase – according to Eq. 15										
${}^0L_{CaO,O}^{liq} = {}^0a_{CaO,O}^{liq} + {}^0b_{CaO,O}^{liq}T$										
${}^0a_{CaO,O}^{liq}$						${}^0b_{CaO,O}^{liq}T$				
-						+30				
Interaction parameter between the Ca and CaO species in the liquid phase – according to Eq. 15										
${}^0L_{Ca,CaO}^{liq} = {}^0a_{Ca,CaO}^{liq} + {}^0b_{Ca,CaO}^{liq}T$										
${}^0a_{Ca,CaO}^{liq}$		${}^0b_{Ca,CaO}^{liq}T$			Note					
-9625		12.30			Accepted, optimized using solubility measurements from Fischbach [47]					
9284		-			<i>Alternative, optimized using activity measurements from Zaitsev et al. [49]</i>					

As discussed in Section 3.5, an alternative description of crystalline CaO using a single Einstein temperature is also proposed in this work. The obtained parameters and the corresponding description of the liquid and amorphous phase are presented in Table 2. The results of the modelling using this alternative description of CaO are very similar to the accepted description above 298.15 K and will not be discussed further in the following sections.

Table 2 – Thermodynamic parameters for an alternative description of crystalline and liquid and amorphous CaO using a single Einstein temperature and only valid from 298.15 K

Alternative description of the Gibbs energy of CaO (crystalline) below its melting point ($298.15 < T < 3222$): $(\text{Ca})_1(\text{O})_1$ – extended Einstein model using a single Einstein temperature, based on Eq. 8					
$G_{(\text{Ca})_1(\text{O})_1}^{\text{cryst}} = E_0 + BT + \frac{6}{2}R\theta_E + 6RT \ln\left(1 - \exp\left(-\frac{\theta_E}{T}\right)\right) - \frac{a}{2}T^2 - \frac{\exp(b + cT)}{c^2}$					
E_0	B	θ_E	a	b	c
-652291.4	-5.1278	445.626	0.00330042	-119.93755	0.00208731
Alternative description of the Gibbs energy of CaO (crystalline) above its melting point ($3222 < T < 6000$): $(\text{Ca})_1(\text{O})_1$ – according to Eq. 10					
$G_{(\text{Ca})_1(\text{O})_1}^{\text{cryst}} = H' - S'T + AT(1 - \ln(T)) + \frac{1}{2C^2(B + CT)}$					
H'	S'	A	B	C	
-730132.6	-491.6656	81.5229	-119.5876	0.04012844	
Alternative description of the Gibbs energy of CaO (amorphous) ($298.15 < T < 6000$): $(\text{CaO})_1$ – based on Eq. 12					
$G_{(\text{CaO})_1}^{\text{am}} = E_0' + BT + \frac{6}{2}R\theta_E + 6RT \ln\left(1 - \exp\left(-\frac{\theta_E}{T}\right)\right) - \frac{a}{2}T^2$					
E_0'	B	θ_E	a		
-617860.5	-5.1278	445.626	0.00330042		
Alternative description of the Gibbs energy of CaO (liquid-amorphous) ($298.15 < T < 6000$): $(\text{CaO})_1$ – according to Eq. 11 and 13					
$G_{(\text{CaO})_1}^{\text{liq-am}} = G_{(\text{CaO})_1}^{\text{am}} - RT \ln\left(1 + \exp\left(-\frac{\Delta G_d}{RT}\right)\right) \text{ with } \Delta G_d = A + BT + CT \ln(T)$					
A		B		C	
27914.1		95.5796		-13.9605	

4. Results and discussion

The results presented in this section were calculated using both Pandat [57] and Thermocalc [50] software packages. The standard thermodynamic properties of the substances modelled in this work are presented in comparison with the relevant literature data in Table 3.

Table 3 – Thermodynamic properties at 298.15 K and 1 bar pressure of the substances modelled in this work compared with the relevant literature data and results from previous modelling

Substance	Reference	C_p° (J.mol ⁻¹ .K ⁻¹)	S° (J.mol ⁻¹ .K ⁻¹)	$\Delta_f H^\circ$ (kJ.mol ⁻¹)
CaO(cr)	This Work – CALPHAD Modelling	42.73	40.35	-634.6
	[18] – CALPHAD Modelling	42.05	38.10	-634.0
	[17] – CALPHAD Modelling	42.02	37.75	-635.1
	[18] – Critical literature review	-	-	-634±1.5
	[24] – DFT calculations	42.73	40.35	-634.6
	[41] – Thermodynamic compilation	42.12	38.21	-635.1
CaO(liq-am)	This Work – CALPHAD Modelling	42.73	40.35	-600.9
	[18] – CALPHAD Modelling	42.04	58.69	-565.6
	[17] – CALPHAD Modelling	42.02	65.69	-555.6
	[41] – Thermodynamic compilation (estimates)	42.12	62.32	-557.3
CaO ₂ (cr)	This Work – CALPHAD Modelling	61.63	59.60	-648.1
	[18] – CALPHAD Modelling	82.84	83.68	-652.7
	[17] – CALPHAD Modelling	82.84	83.68	-659.0
	[24] – DFT calculations	61.58	59.60	-648.1

4.1. Crystalline CaO

The modelled heat content of crystalline CaO are plotted in Fig. 6 along with the available literature data [28-34, 36] and results from previous modellings of the system [17, 18]. A satisfactory fit of all the literature data was obtained, except for the conflicting datasets from Chekhovskoi et al. [34] and Roth et al. [29]. It is highlighted that the data obtained by ab initio molecular dynamics by Alvares et al. [37] serve as a valuable anchor point in the very high temperature range. Indeed, even a slight increase in the heat contents results in a significant increase in the heat capacity as it can be seen when comparing Fig. 6 and Fig. 7 presented below. Compared to previous modellings of the system, the description of Lindberg et al. [17] features a discontinuity in heat content at their selected melting point of 2845 K, and the one of Liang et al. [18] does not reproduce the very high temperature increase in heat content observed experimentally by Chekhovskoi et al. [34] and in molecular dynamics simulations conducted by Alvares et al. [37].

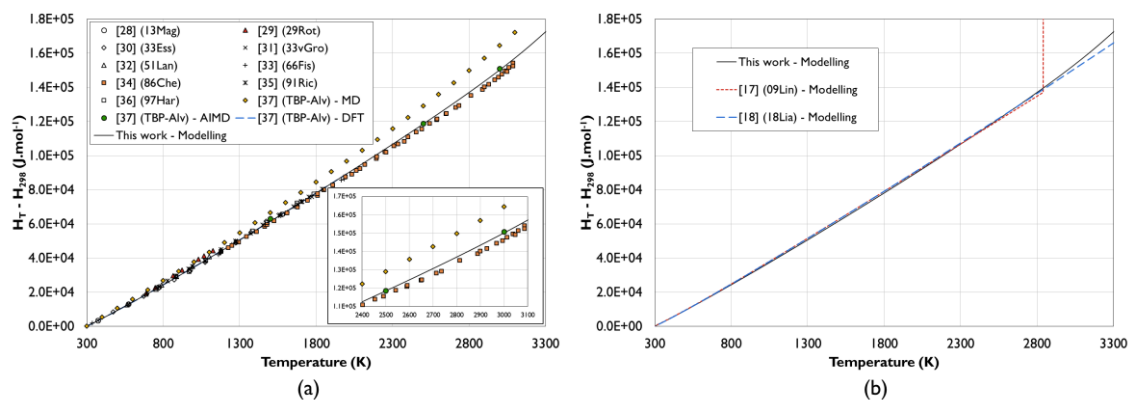


Fig. 6. Modelled heat content of crystalline CaO compared with (a) the literature data (inlet: zoom on the 2400 – 3100 K range) and (b) results from previous modellings of the system

The modelled heat capacity of crystalline CaO is presented along with the available literature data [25-27] and results from previous modellings of the system [17, 18] in Fig. 7. The agreement with the DFT data from Alvares et al. [37] is very satisfying as it is also highlighted in Fig. 4. A very satisfying agreement was also obtained with the experimental data from Parks et al. [26], whereas the data from Gmelin et al. [27] are not fitted closely. Compared to previous modellings of the system, the heat capacity data below 298.15 K cannot be fitted by the latter with 2nd generation models. Besides, both previous descriptions give a less satisfying fit of the DFT data from Pisch et al. [24] on the 350 – 1500 K range. At higher temperatures, the description of Lindberg et al. [17] features an artificial discontinuity at their selected melting point of 2845 K, and the one of Liang et al. [18] does not reproduce the sudden pre-melting increase of heat capacity before the compound's melting point that is a result of the heat content data presented in Fig. 6.

The standard entropy at 298.15 K is calculated from the heat capacity at 40.35 J.mol⁻¹.K⁻¹, which is slightly higher than the value of 38.21 J.mol⁻¹.K⁻¹ compiled in the JANAF tables [41] based on the data from Gmelin et al. [27], as well as the value of 37.75 J.mol⁻¹.K⁻¹ fitted by Lindberg et al. [17] and the one of 38.10 J.mol⁻¹.K⁻¹ fitted by Liang et al. [18].

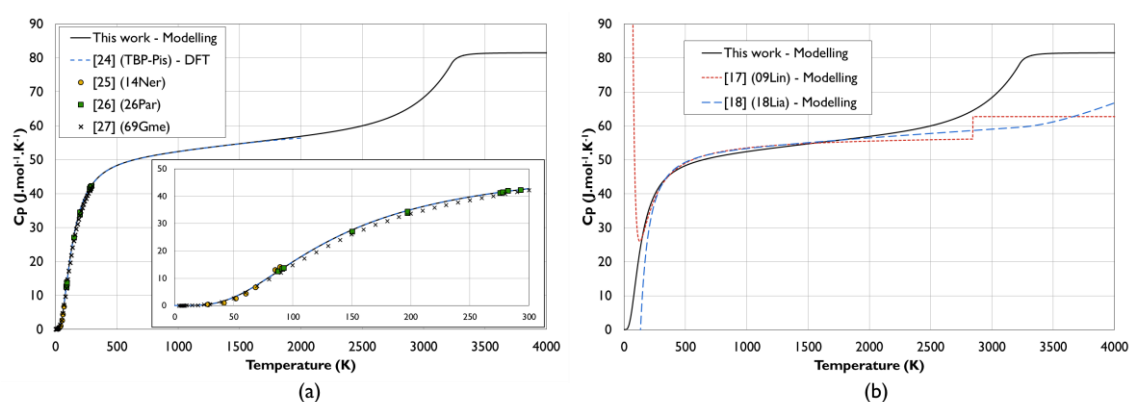


Fig. 7. Modelled heat capacity of crystalline CaO compared with (a) the literature data (inlet: zoom on the 0 – 300 K range) and (b) results from previous modellings of the system. It is noted that although the heat capacity modelled in previous assessments are plotted on the whole temperature range, their validity range was suggested by the authors to be limited below 298.15 K and above 3500 K in the case of Lindberg et al. [17].

The standard enthalpy of formation of CaO is modelled at -634.6 kJ.mol⁻¹ (-317.3 kJ.mol of atoms⁻¹) which is in perfect agreement with the DFT calculations Pisch et al. [24] and in a very satisfying agreement with the value of -634±1.5 kJ.mol⁻¹ critically assessed from the experimental literature by Liang et al. [23] as well as the value assessed in the JANAF compilation [41] of -635.09±0.88 kJ.mol⁻¹. Therefore no significant differences are obtained between the enthalpy of formation fitted in this work and the ones of -635.09 kJ.mol⁻¹ and -634.00 kJ.mol⁻¹ fitted by Lindberg et al. [17] and Liang et al. [18] respectively.

4.2. Liquid and amorphous CaO

The modelled heat capacity of liquid and amorphous CaO is presented on Fig. 8 along with the data obtained by Alvares et al. [37].

On Fig. 8 (a) is also presented for comparison a tentative modelling of the phase using a non-zero residual entropy at 0 K taken at an arbitrary value of 3 J.mol⁻¹.K⁻¹ as well as the modelled heat capacity of crystalline CaO. In both tentative modellings of the liquid and amorphous phase, the thermodynamic properties at the selected melting point of 3222 K are almost identical. Using a non-zero residual entropy enable to ensure that the entropy of the liquid is always strictly higher than the entropy of the crystalline phase. At the melting point, the Gibbs energy contribution of the residual entropy is then minus 3 times 3222 K, that is to say roughly -9.7 kJ.mol⁻¹. For the tentative modelling with a non-zero residual entropy to fit the same fixed melting point and enthalpy of fusion, the non-residual entropy has therefore to be lower at 3222 K. This is obtained by a shift of the heat capacity increase towards high temperatures. By roughly estimating the glass transition temperature at the

half of the heat capacity increase, a temperature of 1150 K is obtained without residual entropy compared to 1275 K when adding a residual entropy of $3 \text{ J}\cdot\text{mol}^{-1}\cdot\text{K}^{-1}$ at 0 K. The description of the liquid and amorphous CaO accepted in this work is the one without residual entropy, notably as no data are available on the glass transition and it gave a slightly more satisfying fit of the data from Alvares et al. [37]. It might be interesting to investigate on the impact of the residual entropy on the goodness of fit for a compound for which the thermodynamic properties are very well established.

On Fig. 8 (b), the accepted description of liquid and amorphous CaO, that is to say the one without residual entropy at 0 K, is compared with the results from previous modellings of the system [17, 18]. It is noted that Lindberg et al. [17] used the exact same description of the heat capacity for solid and liquid CaO. The heat capacity of liquid CaO modelled by Liang et al. [18] is in acceptable agreement with the one proposed in this work above the melting point of CaO selected at 3222 K in both assessments. Below the melting point however, the description of the metastable liquid phase proposed by Liang et al. [18] does not feature the expected increase in heat capacity with the decreasing temperature.

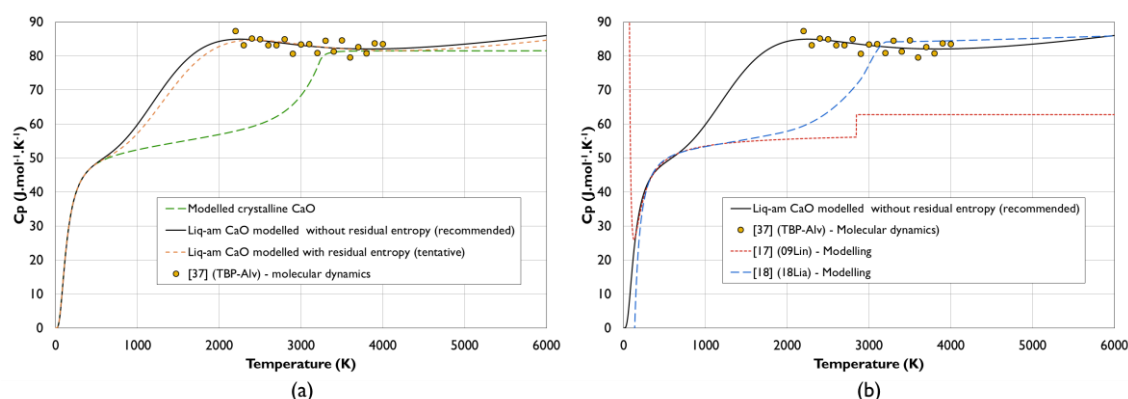


Fig. 8. Modelled heat capacity of liquid and amorphous CaO along with the available literature data. In (a), the accepted description is compared with a tentative description of the phase with a residual entropy of $3 \text{ J}\cdot\text{mol}^{-1}\cdot\text{K}^{-1}$ as well as with the modelled heat capacity of crystalline CaO. In (b), the accepted description is compared with results from previous modellings of the system. It is noted that although the heat capacity modelled in previous assessments are plotted on the whole temperature range, their validity range was suggested by the authors to be limited below 298.15 K and above 3500 K in the case of Lindberg et al. [17].

The selected melting point of CaO at 3222 K based on the work of Manara et al. [19] was perfectly fitted, and the modelled enthalpy of fusion of $81.1 \text{ kJ}\cdot\text{mol}^{-1}$ is in good agreement with the value of $80.92 \text{ kJ}\cdot\text{mol}^{-1}$ calculated by Alvares et al. [37] as well as with the value of $80\pm 16 \text{ kJ}\cdot\text{mol}^{-1}$ estimated by Gurvich et al. [43]. The corresponding modelled entropy of fusion is $25.2 \text{ J}\cdot\text{mol}^{-1}\cdot\text{K}^{-1}$. The heat content at 3200 K when taking for reference the enthalpy of crystalline CaO at 298.15 K was modelled at $245.6 \text{ kJ}\cdot\text{mol}^{-1}$, which is in good agreement with the value of $248.2 \text{ kJ}\cdot\text{mol}^{-1}$ obtained by ab initio molecular dynamics by Alvares et al. [37].

The standard enthalpy of formation of liquid and amorphous CaO is modelled at $-600.9 \text{ kJ}\cdot\text{mol}^{-1}$ ($-300.5 \text{ kJ}\cdot\text{mol}^{-1}$ of atoms⁻¹), which is $33.7 \text{ kJ}\cdot\text{mol}^{-1}$ less exothermic than the one obtained for crystalline CaO. The standard entropy of the liquid and amorphous phase is equal to the one of crystalline CaO, that is to say $40.35 \text{ J}\cdot\text{mol}^{-1}\cdot\text{K}^{-1}$. This result directly comes from the fact that, in the absence of data, the heat capacity of amorphous CaO was taken equal to the one of the crystalline phase, and no residual entropy was added at 0 K in the accepted description of the phase.

4.3. Crystalline CaO₂

The modelled heat capacity of crystalline CaO₂ is presented in Fig. 9 along with the DFT data from Pisch et al. [24] and the results from previous modellings of the system [17, 18]. A very satisfying agreement was obtained up to 298.15 K as it can also be seen on Fig. 5. The standard entropy of the phase is calculated from the heat capacity function at $59.6 \text{ J}\cdot\text{mol}^{-1}\cdot\text{K}^{-1}$. At higher temperature, the heat capacity tends to a constant value of $3R$ per

atoms. The proposed description presents an obvious improvement compared to the constant heat capacity of $82.8 \text{ J}\cdot\text{mol}^{-1}\cdot\text{K}^{-1}$ selected in previous modellings of the system [17, 18].

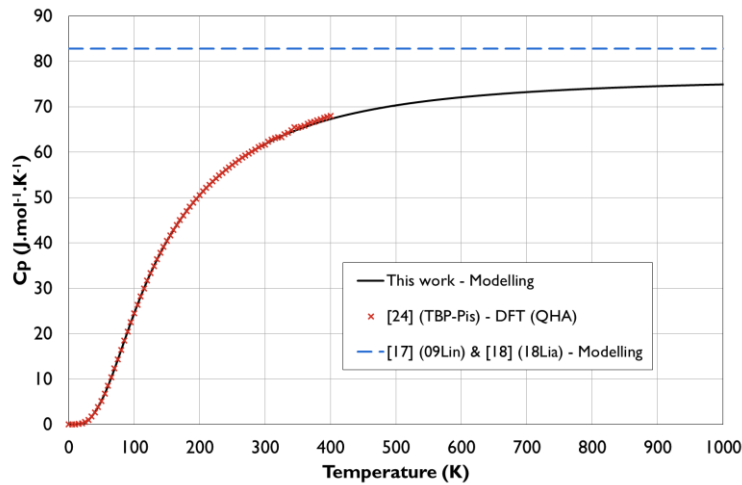


Fig. 9. Modelled heat capacity of crystalline CaO_2 along with the literature data and results from previous modellings of the system

The standard enthalpy of formation of CaO_2 is modelled at $-648.1 \text{ kJ}\cdot\text{mol}^{-1}$ ($-216.0 \text{ kJ}\cdot\text{mol}$ of atoms $^{-1}$) which is in perfect agreement with the only available literature data obtained from DFT calculations by Pisch et al. [24].

4.4. The Ca – O phase diagram

First of all, it is reminded that after discarding the result from Bevan et al. [46] and the solubility data reported by Zaitsev et al. [49], two datasets with conflicting trends remain available in the literature related to the Ca – CaO liquidus, that is to say the solubility measurements from Fischbach [47] and the activity data from Zaitsev et al. [49]. Both these conflicting datasets were fitted in two separate attempts. The modelled Ca – CaO liquidus and activity of Ca in the liquid phase are presented for the two resulting attempts along with experimental data in Fig. 10. The whole Ca – CaO liquidus with the gas phase suspended in the calculations are compared for both different versions in Fig. 11.

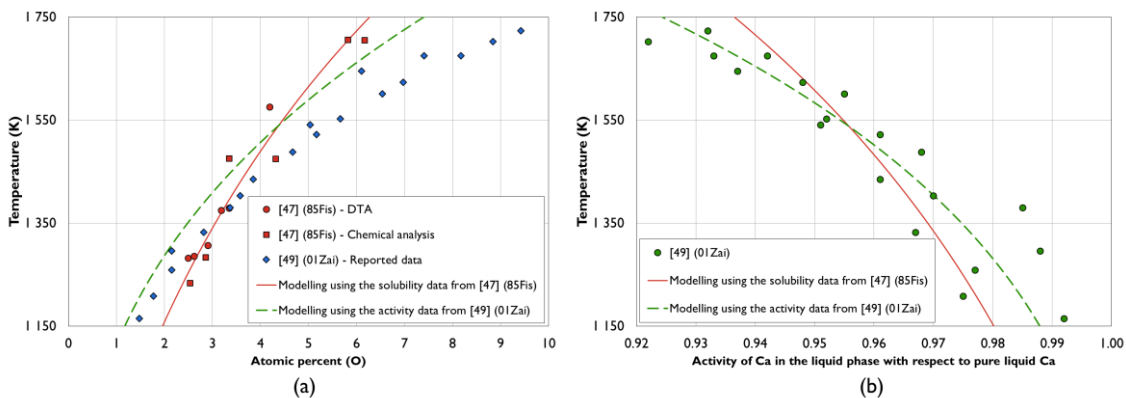


Fig. 10. Comparison between the fit obtained with three different modellings of the interaction between Ca and CaO in the liquid phase and (a) the available data on the Ca – CaO liquidus, and (b) the activity of Ca in the liquid phase with reference to liquid Ca taken at the temperature of the calculation. It is noted that the solubility data reported by Bevan et al. [46] is not presented on (a) in order to allow a better resolution. Also, although the gas phase does not appear as a stable in this temperature range under 1 bar of pressure, it is noted that it was suspended in the calculations.

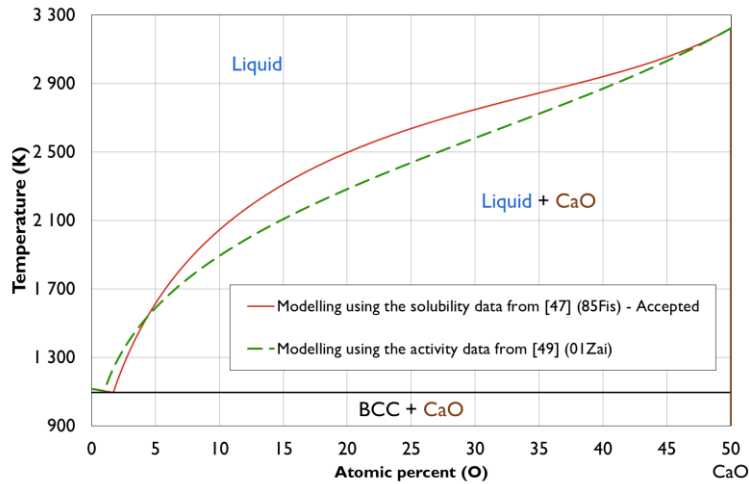


Fig. 11. Comparison between the Ca – CaO liquidus obtained with two different modellings of the interactions between Ca and CaO in the liquid phase. The gas phase was suspended in the calculations.

It is highlighted from Fig. 10 and 11 that although the solubility measurements from Fischbach [47] and the activity measurements from Zaitsev et al. [49] are in an acceptable agreement in the 1150 – 1750 K range, they both features conflicting trends that lead to significant differences in the higher temperature range. In fact, the interaction between Ca and CaO in the liquid phase are found to be always repulsive and constant with the temperature when fitting the activity data from Zaitsev et al. [49], whereas when taking the liquidus data from Fischbach [47] the interactions are found to be attractive up to 783 K and increasingly repulsive from this point.

At higher temperatures, the potential existence of a miscibility gap in the Ca – CaO liquid was suggested by Bevan and Richardson [46], and this possibility was left open by Wriedt [10] in his assessment of the system. None of the modelled liquidus feature a miscibility gap, although the "S-shaped" curvature obtained when fitting the data from Fischbach [47] suggests a slight tendency to demixing.

Regarding the eutectic between β -Ca and CaO, the results obtained with both different versions of the modelling are presented in Table 4. Results from the modelling based on the activity data from Zaitsev et al. [49] is in a slightly better agreement with eutectic temperature estimated from the literature data to roughly lie between 1105 K and 1114 K.

Table 4 – Modelled eutectic between β -Ca and CaO for the two different versions of the Ca – O system investigated in this section

Temperature in K	Composition of the invariant point in at.%O	Note
1094.6	1.70	Modelling using the solubility data from [47] (85Fis) - Accepted
1103.2	0.98	Modelling using the activity data from [49] (01Zai)

In this work, the modelling based on the direct liquidus measurements from Fischbach [47] is accepted over the one based on the activity data from Zaitsev et al. [49]. As it was argued in the review of the literature, the latter measurements represent more delicate experimental work, whereas the validity of the former are supported by the consistency between the datasets obtained with two different experimental techniques and by the experimental rigour of the author.

The modelled Ca – O diagram calculated at 1 bar is presented in Fig. 12.

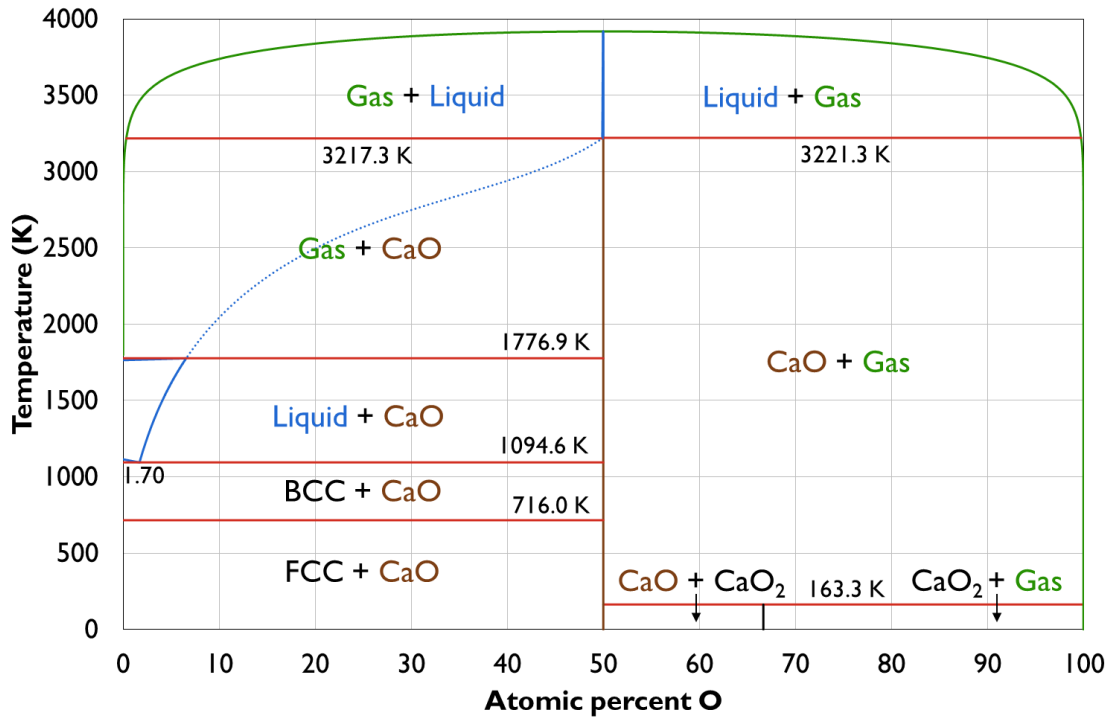


Fig. 12. The Ca – O phase diagram calculated in this work under the pressure of 1 bar. The Ca – CaO liquidus extended up to the melting of CaO is obtained by suspending the gas phase from the calculation and is represented by a blue dotted line.

The CaO₂ phase is predicted to decompose at 163 K under 1 bar of pressure, which is quite lower than the temperature of roughly 300 K reviewed by Wriedt [10]. As mentioned before, pure CaO₂ may not exist and is merely an oxide-hydroxide mixture with attached water [44], which is in agreement with our modelling and would explain the wrongly estimated data in the literature. It is reminded here that to ensure the validity of the calculations, the Gibbs energy function of O_{2(g)} was extended down to 100 K by keeping the heat capacity constant from 298.15 K as suggested in the JANAF tables [41]. It is noted however that this correction had only a limited effect on the results of the calculations. Indeed, the difference in the calculated decomposition temperature of CaO₂ was less than 0.3 K down to the pressure of 10⁻⁵ bar where the invariant is calculated to occur at 104 K.

CaO is predicted to melt congruently down to 0.05 bar of pressure. The corresponding temperature of 3221.9 K differ only very slightly from the temperature of 3222.0 K modelled in the pseudo-unary due to the presence of roughly 0.001 mole percent of Ca and O in the associate liquid at the melting point.

In order to discuss the melting of CaO in more details, a zoom in the zone of interest is presented in Fig. 13. This part of the Ca – O diagram was calculated under a pressure of 0.63 bar in order to be consistent with the measurements from Manara et al. [19] performed under compressed air at 0.3 MPa of pressure. Under those conditions, a decomposition temperature of 3222±25 K was measured by the authors. By comparing their data with the melting point measured at 3178 K by Yamada et al. [58] under 0.1 MPa of air, it was assumed by Manara et al. [19] that CaO was stabilized up to its congruent melting point in both experiments, and that under oxidizing conditions the variation of the melting point of CaO over a pressure variation of a few tenths of MPa should be negligible. Therefore, it is assumed that the invariant decomposition of CaO on the oxygen-rich side to form liquid CaO and an oxygen-rich gas should match closely the congruent melting point of CaO and should not vary significantly over a few tenths of MPa of pressure. In order to meet this assumption, an interaction parameter of +30.T taken from the modelling performed by Liang et al. [18] was added between CaO and O in the liquid phase. Using this parameter, the non-congruent melting of CaO is unchanged in the calcium-rich side, and in the oxygen-rich side the solidification point under 0.63 bar is predicted at 3221.5 K instead of 3203 K

without it. Besides, it is noted that in a reducing environment (Ar + 6% H₂ at 0.3 MPa), Manara et al. [19] systematically obtained a lower solidification point of 3192±40 K when compared with the temperature of 3222±25 K measured in an oxidizing environment (0.3 MPa of air). As a result of the interaction parameter added between CaO and O in the liquid phase, the invariant decomposition of CaO in the Ca-rich side is always lower in temperature than the one is the O-rich side. Nonetheless, the measurement performed by Manara et al. [19] in a reducing environment cannot reasonably be used in the modelling as the experimental Ca and O partial pressures are unknown. Indeed, it is noted that the non-congruent melting temperature of CaO in the calcium-rich side is predicted to vary significantly with the pressure, ranging from 3222 K under 0.1 bar of pressure to 3168 K under 10 bar.

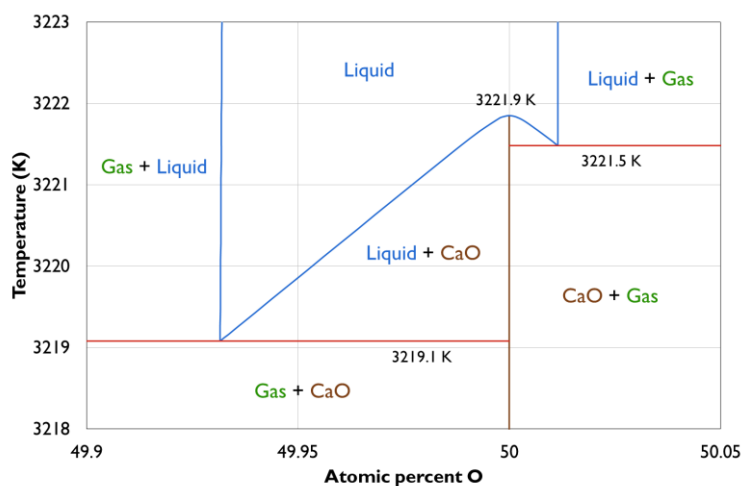


Fig. 13. The melting of CaO under 0.63 bar of pressure

Conclusions

In this work, a thermodynamic description of the Ca – O system is proposed, including 3rd generation description of crystalline CaO, liquid and amorphous CaO, and crystalline CaO₂.

The present modelling is notably based on recent information provided by DFT [24] and coupled DFT and molecular dynamics [37] investigations which enable a much more robust description of the thermodynamic properties of the binary phases. Indeed, in a literature review the mentioned calculations were found to be in a very satisfying agreement with the experimental data for which a consensus was already achieved, such as for the heat content of crystalline CaO, and enabled a critical selection of the data for which conflicting values were reported. For instance, the low temperature heat capacity of crystalline CaO was reassessed, and a standard entropy of 40.35 J.mol⁻¹.K⁻¹ consistent with the experimental work from Park et al. [26] was preferred compared to the value of 38.21 J.mol⁻¹.K⁻¹ accepted so far and based on the only measurements available on the whole low temperature range [40]. In addition, the mentioned DFT calculations and molecular dynamics simulations provided data in areas that are hardly accessible to experiments, enabling an improved description of crystalline CaO₂ as well as of liquid and amorphous CaO.

Besides, it is highlighted here that a satisfactorily fit of the high temperature heat content data selected for crystalline CaO could not be obtained using the additional parameters given in terms of polynomial functions of temperature used so far in the 3rd generation models. It is suggested that those terms are not suited to describe the thermodynamic properties of refractory oxides in general. In this work, new terms in the form of $T_{exp}(A+BT)$ or $T/(A+BT)^3$ are proposed instead. In the present case, they were proven to allow a much greater flexibility in describing the heat capacity of crystalline CaO up to the melting point in a single expression, while also resulting in numerically reasonable values for the parameters.

In addition, it is emphasized that a satisfactorily fit of the thermodynamic properties of crystalline CaO could not be obtained using an extended Einstein model with a single Einstein temperature. Indeed, because a poor fit is

obtain in the low temperature range, the heat capacity value and trend at 298.15 K had to diverge from with the selected data in order to be able to fit the standard entropy of the phase. As a result, the extra terms originally added in the model to account for non-thermodynamic information had to be used to make up for it, leading to a less satisfying fit in the whole temperature range.

In order to make the modelling of the Ca – O more robust, measurements of the Ca/CaO eutectic as well as of the solubility of CaO in liquid Ca in the 1150 – 1250 K range would serve as valuable anchor points for the liquid phase, and would therefore be interesting experimental perspectives. In addition, 3rd generation modelling of the Ca and O unary systems would be valuable inputs in the proposed modelling.

Acknowledgements and data availability

Financial support for this study was provided in the frame of the "OPALHE" project in the "Institut Carnot - Energie du Future" program. Fruitful discussions within the French collaborative network in high temperature thermodynamics GDR CNRS 3584 (TherMatHT) as well as with Prof. Rainer Schmid-Fetzer (TU Clausthal) are also acknowledged. Financial support is also acknowledged from the research network Nanocem (www.nanocem.org) in the frame of the core project "High-temperature thermodynamics of Portland Cement Clinkers". Last but not least, CIMENT/GRICAD is acknowledged for computational resources.

The data required to reproduce these findings are available as supplementary material in the form of two thermodynamic database files.

References

- [1] M.W. Chase, I. Ansara, A. Dinsdale, G. Eriksson, G. Grimvall, L. Höglund, H. Yokokawa, Workshop on thermodynamic models and data for pure elements and other endmembers of solutions: Schloß Ringberg, Feb. 26 to March 3, 1995, *Calphad*, 19 (1995) 437-447, [https://doi.org/10.1016/0364-5916\(96\)00002-8](https://doi.org/10.1016/0364-5916(96)00002-8).
- [2] J. Ågren, B. Cheynet, M.T. Clavaguera-Mora, K. Hack, J. Hertz, F. Sommer, U. Kattner, Workshop on thermodynamic models and data for pure elements and other endmembers of solutions: Schloß Ringberg, Febr. 21, to March 3, 1995, *Calphad*, 19 (1995) 449-480, [https://doi.org/10.1016/0364-5916\(96\)00003-X](https://doi.org/10.1016/0364-5916(96)00003-X).
- [3] A.V. Khvan, T. Babkina, A.T. Dinsdale, I.A. Uspenskaya, I.V. Fartushna, A.I. Druzhinina, A.B. Syzdykova, M.P. Belov, I.A. Abrikosov, Thermodynamic properties of tin: Part I Experimental investigation, ab-initio modelling of α -, β -phase and a thermodynamic description for pure metal in solid and liquid state from 0 K, *Calphad*, 65 (2019) 50-72, <https://doi.org/10.1016/j.calphad.2019.02.003>.
- [4] S. Bigdeli, Q. Chen, M. Selleby, A New Description of Pure C in Developing the Third Generation of Calphad Databases, *Journal of Phase Equilibria and Diffusion*, 39 (2018) 832-840, 10.1007/s11669-018-0679-3.
- [5] A.V. Khvan, A.T. Dinsdale, I.A. Uspenskaya, M. Zhilin, T. Babkina, A.M. Phiri, A thermodynamic description of data for pure Pb from 0K using the expanded Einstein model for the solid and the two state model for the liquid phase, *Calphad*, 60 (2018) 144-155, <https://doi.org/10.1016/j.calphad.2017.12.008>.
- [6] Z. Li, S. Bigdeli, H. Mao, Q. Chen, M. Selleby, Thermodynamic evaluation of pure Co for the third generation of thermodynamic databases, *physica status solidi (b)*, 254 (2017) 1600231, 10.1002/pssb.201600231.
- [7] S. Bigdeli, H. Mao, M. Selleby, On the third-generation Calphad databases: An updated description of Mn, *physica status solidi (b)*, 252 (2015) 2199-2208, 10.1002/pssb.201552203.
- [8] C.A. Becker, J. Ågren, M. Baricco, Q. Chen, S.A. Decterov, U.R. Kattner, J.H. Perepezko, G.R. Pottlacher, M. Selleby, Thermodynamic modelling of liquids: CALPHAD approaches and

- contributions from statistical physics, *physica status solidi (b)*, 251 (2014) 33-52, 10.1002/pssb.201350149.
- [9] Q. Chen, B. Sundman, Modeling of thermodynamic properties for Bcc, Fcc, liquid, and amorphous iron, *Journal of Phase Equilibria*, 22 (2001) 631-644, 10.1007/s11669-001-0027-9.
- [10] H.A. Wriedt, The Ca–O (Calcium-Oxygen) system, *Bulletin of Alloy Phase Diagrams*, 6 (1985) 337-342, 10.1007/bf02880517.
- [11] H.F.W. Taylor, *Cement chemistry*, 2nd Edition, Thomas Telford 1997, 10.1680/cc.25929.
- [12] C. Le Losq, D.R. Neuville, Molecular structure, configurational entropy and viscosity of silicate melts: Link through the Adam and Gibbs theory of viscous flow, *Journal of Non-Crystalline Solids*, 463 (2017) 175-188, <https://doi.org/10.1016/j.jnoncrysol.2017.02.010>.
- [13] M. Reuter, Y. Xiao, U. Boin, Recycling and environmental issues of metallurgical slags and salt fluxes, VII International Conference on Molten Salts Fluxes and Salts, The South African Institute of Mining and Metallurgy, (2004),
- [14] S. Takahashi, D.R. Neuville, H. Takebe, Thermal properties, density and structure of percalcic and peraluminous CaO–Al₂O₃–SiO₂ glasses, *Journal of Non-Crystalline Solids*, 411 (2015) 5-12, <https://doi.org/10.1016/j.jnoncrysol.2014.12.019>.
- [15] C.W. Bale, E. Bélisle, P. Chartrand, S.A. Decterov, G. Eriksson, A.E. Gheribi, K. Hack, I.H. Jung, Y.B. Kang, J. Melançon, A.D. Pelton, S. Petersen, C. Robelin, J. Sangster, P. Spencer, M.A. Van Ende, FactSage thermochemical software and databases, 2010–2016, *Calphad*, 54 (2016) 35-53, <https://doi.org/10.1016/j.calphad.2016.05.002>.
- [16] M. Hillert, M. Selleby, B. Sundman, An assessment of the Ca-Fe-O system, *Metallurgical Transactions A*, 21 (1990) 2759-2776, 10.1007/bf02646071.
- [17] D. Lindberg, P. Chartrand, Thermodynamic evaluation and optimization of the (Ca+C+O+S) system, *The Journal of Chemical Thermodynamics*, 41 (2009) 1111-1124, <https://doi.org/10.1016/j.jct.2009.04.018>.
- [18] S.-M. Liang, R. Schmid-Fetzer, Complete thermodynamic description of the Mg-Ca-O phase diagram including the Ca-O, Mg-O and CaO-MgO subsystems, *Journal of the European Ceramic Society*, 38 (2018) 4768-4785, <https://doi.org/10.1016/j.jeurceramsoc.2018.06.015>.
- [19] D. Manara, R. Böhler, L. Capriotti, A. Quaini, Z. Bao, K. Boboridis, L. Luzzi, A. Janssen, P. Pöml, R. Eloirdi, R.J.M. Konings, On the melting behaviour of calcium monoxide under different atmospheres: A laser heating study, *Journal of the European Ceramic Society*, 34 (2014) 1623-1636, <https://doi.org/10.1016/j.jeurceramsoc.2013.12.018>.
- [20] K.V. Gourishankar, M.K. Ranjbar, G.R.S. Pierre, Revision of the enthalpies and gibbs energies of formation of calcium oxide and magnesium oxide, *Journal of Phase Equilibria*, 14 (1993) 601-611, 10.1007/bf02669141.
- [21] E.J. Huber, C.E. Holley, The Heat of Combustion of Calcium, *The Journal of Physical Chemistry*, 60 (1956) 498-499, 10.1021/j150538a026.
- [22] F.D. Rossini, D.D. Wagman, W.H. Evans, S. Levine, I. Jaffe, Selected values of chemical thermodynamic properties : Circular of the National Bureau of Standards 500, U.S. Government Printing Office, (1952),
- [23] S.-M. Liang, A. Kozlov, R. Schmid-Fetzer, The Mg–Ca–O system: Thermodynamic analysis of oxide data and melting/solidification of Mg alloys with added CaO, *International Journal of Materials Research*, 109 (2018) 185-200, 10.3139/146.111596.
- [24] A. Pisch, G. Deffrennes, A. Pasturel, Thermodynamics of alkaline earth oxides using DFT, (TBP),
- [25] W. Nernst, F. Schwers, Untersuchungen über die spezifische Wärme bei tiefen Temperaturen, *Ber. Kgl. Pr. Akad. Wiss.*, 10 (1914) 355-370,
- [26] G.S. Parks, K.K. Kelley, The Heat Capacities of Some Metallic Oxides, *The Journal of Physical Chemistry*, 30 (1926) 47-55, 10.1021/j150259a005.
- [27] E. Gmelin, Thermal Properties of Alkaline-Earth-Oxides, *Z. Naturforsch.*, 24 a (1969) 1794 - 1800,
- [28] A. Magnus, Specific heat measurements of stable solids at high temperatures, *Phys. Z.*, 14 (1913) 5 - 11,

- [29] W.A. Roth, W. Bertram, Measurements of the Specific Heat of Metallurgically Important Substances in a Large Temperature Interval with Help of Two New Calorimeter Types, *Z. Elektrochem.*, 35 (1929) 297 - 308,
- [30] H. Esser, K. Averdick, W. Grass, Wärmeinhalt einiger Metalle, Legierungen und Schlackenbildner bei Temperaturen bis 1200°, *Archiv für das Eisenhüttenwesen*, 6 (1933) 289-292, 10.1002/srin.193300418.
- [31] H.E. von Gronow, H.E. Schwiete, Die spezifischen Wärmen von CaO, Al₂O₃, CaO·Al₂O₃, 3CaO·Al₂O₃, 2CaO·SiO₂, 3CaO·SiO₂, 2CaO·Al₂O₃·SiO₂ von 20° bis 1500° C, *Zeitschrift für anorganische und allgemeine Chemie*, 216 (1933) 185-195, 10.1002/zaac.19332160212.
- [32] J.J. Lander, Experimental Heat Contents of SrO, BaO, CaO, BaCO₃ and SrCO₃ at High Temperatures. Dissociation Pressures of BaCO₃ and SrCO₃, *Journal of the American Chemical Society*, 73 (1951) 5794-5797, 10.1021/ja01156a094.
- [33] W.A. Fischer, W. Ertmer, Die Bestimmung des Wärmeinhalts und der spezifischen Wärme von Schmelzkalkkristallen zwischen 0 und 1720 °C, *Archiv für das Eisenhüttenwesen*, 37 (1966) 275-281, 10.1002/srin.196602760.
- [34] V.Y. Chekhovskoi, K. Irgashov, V.D. Tarasov, Experimental investigation of the enthalpy and heat capacity of calcium oxides up to the temperature 3100K (in Russian), *Teplofiz. Vys. Temp.*, 24 (1986) 614,
- [35] P. Richet, G. Fiquet, High-temperature heat capacity and premelting of minerals in the system MgO-CaO-Al₂O₃-SiO₂, *Journal of Geophysical Research: Solid Earth*, 96(B1) (1991) 445-456, <https://doi.org/10.1029/90JB02172>.
- [36] S. Hara, Measurement of heat contents of oxides at elevated temperature using a drop calorimeter, *Koon gakkaiishi*, 23 (1997) 25 - 30,
- [37] C.M.S. Alvares, G. Deffrennes, A. Pisch, N. Jakse, Thermodynamics and structural properties of CaO: A molecular dynamics simulations study, Submitted to *Journal of Chemical Physics*,
- [38] A. Pisch, A. Pasturel, G. Deffrennes, O. Dezellus, P. Benigni, G. Mikaelian, Investigation of the thermodynamic properties of Al₄C₃: A combined DFT and DSC study, *Computational Materials Science*, 171 (2020) 109100, <https://doi.org/10.1016/j.commatsci.2019.109100>.
- [39] J. Sun, A. Ruzsinszky, J.P. Perdew, Strongly Constrained and Appropriately Normed Semilocal Density Functional, *Physical Review Letters*, 115 (2015) 036402, 10.1103/PhysRevLett.115.036402.
- [40] E. Gmelin, Mesures de la chaleur spécifique de l'oxyde de béryllium et de l'oxyde de calcium à basses températures, *C. R. Acad. Sc. Paris, Série C*, 262 (1966) 1452,
- [41] M.W. Chase, NIST-JANAF Thermochemical Tables, Fourth Edition, *Journal of Physical and Chemical Reference Data*, Monograph 9 (Part I and Part II), (1998) 1963,
- [42] P. Richet, J. Ingrin, B.O. Mysen, P. Courtial, P. Gillet, Premelting effects in minerals: an experimental study, *Earth and Planetary Science Letters*, 121 (1994) 589-600, [https://doi.org/10.1016/0012-821X\(94\)90093-0](https://doi.org/10.1016/0012-821X(94)90093-0).
- [43] L.V. Gurvich, L.V. Veyts, C.B. Alcock, *Thermodynamic Properties of Individual Substances*, CRC Press, 3 (1994),
- [44] C. Brosset, N.-G. Vannerberg, Formation of Calcium Superoxide, *Nature*, 177 (1956) 238-238, 10.1038/177238a0.
- [45] I. Barin, *Thermochemical Data of Pure Substances*, Third Edition, VCH Publishers, New York, (1995),
- [46] D.J.M. Bevan, F.D. Richardson, The Solution Of Lime and Liquid Calcium and its Effect on the Reducing Properties of the Metal, *Proc. Australian At. En. Symp. on the Peaceful Uses of At. En.* 1958, Melbourne University Press, (1959) 586-587,
- [47] H. Fischbach, Thermodynamic data for liquid Ca-CaF₂ and Ca-CaCl₂ slags, *Steel Research*, 56 (1985) 365-368, 10.1002/srin.198500649.
- [48] A.I. Zaitsev, N.V. Korolev, N.P. Lyakishev, B.M. Mogutnov, Thermodynamic Properties and Phase Equilibria in the Ca-CaO System, *Russian Journal of Inorganic Chemistry*, 45 (2000) 1121 - 1123,
- [49] A.I. Zaitsev, B.M. Mogutnov, Thermodynamics of the Ca-CaO-CaF₂ system, *Metallurgical and Materials Transactions B*, 32 (2001) 305-311, 10.1007/s11663-001-0053-3.

- [50] J.O. Andersson, T. Helander, L. Höglund, P. Shi, B. Sundman, Thermo-Calc & DICTRA, computational tools for materials science, *Calphad*, 26 (2002) 273-312, [https://doi.org/10.1016/S0364-5916\(02\)00037-8](https://doi.org/10.1016/S0364-5916(02)00037-8).
- [51] J. Ågren, Thermodynamics of Supercooled Liquids and their Glass Transition, *Physics and Chemistry of Liquids*, 18 (1988) 123-139, 10.1080/00319108808078586.
- [52] J.W.P. Schmelzer, T.V. Tropin, Glass Transition, Crystallization of Glass-Forming Melts, and Entropy, *Entropy*, 20 (2018), <https://doi.org/10.3390/e20020103>.
- [53] H.S. Krull, R.N. Singh, F. Sommer, Generalized association model, *Z. Metallkd.*, 91 (2000) 356 - 365,
- [54] F. Sommer, Association Model for the Description of the Thermodynamic Functions of Liquid Alloys - Basic Concepts, *Z. Metallkd.*, 73 (1982) 72 - 86,
- [55] A.T. Dinsdale, SGTE data for pure elements, *Calphad*, 15 (1991) 317-425, [https://doi.org/10.1016/0364-5916\(91\)90030-N](https://doi.org/10.1016/0364-5916(91)90030-N).
- [56] SGTE, SGTE Substance Database (SGSUB), accessed 06 december 2019, <https://www.sgte.net/en/thermochemical-databases>,
- [57] W. Cao, S.L. Chen, F. Zhang, K. Wu, Y. Yang, Y.A. Chang, R. Schmid-Fetzer, W.A. Oates, PANDAT software with PanEngine, PanOptimizer and PanPrecipitation for multi-component phase diagram calculation and materials property simulation, *Calphad*, 33 (2009) 328-342, <https://doi.org/10.1016/j.calphad.2008.08.004>.
- [58] T. Yamada, M. Yoshimura, S. Somiya, Reinvestigation of the solidification point of CaO by digital pyrometry, *Journal of the American Ceramic Society*, 69 (1986) C-243-C-245, doi:10.1111/j.1151-2916.1986.tb07350.x.